Available online at www.sciencedirect.com
SCIENCE DIRECT
Precambrian Research 148 (2006) 125–144
Precambrian Research
www.elsevier.com/locate/precamres

The uranium mineralization potential of the Paleoproterozoic Sioux Basin and its relationship to other basins in the southern Lake Superior region

Adrienne J. Hanly [a,*], T. Kurtis Kyser [a], Eric E. Hiatt [b], Jim Marlatt [c], Sandra Foster [c]

[a] *Department of Geological Sciences and Geological Engineering, Queen's University, Kingston, Ont., Canada K7L 3N6*
[b] *Geology Department, University of Wisconsin, 800 Algoma Boulevard, Oshkosh, WI 54901, USA*
[c] *Cameco Corporation, 2121-11th Street West, Saskatoon, Sask., Canada S7M 1J3*

Received 19 June 2005; received in revised form 14 March 2006; accepted 22 March 2006

Abstract

The Paleoproterozoic Sioux Basin and the Baraboo, Barron, Flambeau, McCaslin, and Waterloo quartzites in northcentral USA are all supermature quartz arenites that are among the world's oldest redbeds. These quartzites were deposited on a stable craton at ca. 1750 Ma, following exhumation and uplift of Penokean crust and major orogenic activity related to the amalgamation of Archean microcontinents at ca. 2.0–1.8 Ga to form Laurentia. $^{40}Ar/^{39}Ar$ ages of 1615–1543 Ma from diagenetic muscovite in the Sioux Basin provide the first geochronological evidence for Mazatzal-related deformation and low-grade metamorphism of the quartzites during subsequent convergence on the southern margin of Laurentia. One muscovite sample from the Sioux Basin has a $^{40}Ar/^{39}Ar$ age of 1465 Ma that likely corresponds with fluid and thermal resetting due to felsic magmatism in the region and is similar to $^{40}Ar/^{39}Ar$ ages for muscovite from the Baraboo and Waterloo quartzites. Thus, the Sioux Basin and other quartzites in the region have experienced a similar tectonic and fluid history.

The Sioux Basin has similar sedimentologic characteristics as other Paleoproterozoic basins in North America, including the uranium-rich Athabasca Basin, Canada, that is host to some of the world's largest and highest-grade unconformity-type uranium deposits. We compared key characteristics, such as the stratigraphy, character of diagenetic fluids, paleoaquifer characteristics, and composition of leachable Pb in the sandstones from the Sioux Basin with the Athabasca Basin in order to evaluate the fluid history of the basin and the potential of the Sioux Basin to host unconformity-type uranium mineralization. Based on the hydrogen and oxygen isotopic composition of muscovite (M1) that formed during diagenesis at 150–200 °C, the pore fluids that were present during peak diagenesis in the Sioux Basin had $\delta^{18}O$ and δD values of −0.5 to +5.2‰ and −32 to −46‰, respectively, similar to those of the fluids associated with uranium mineralization and alteration in the Athabasca Basin. However, fluid flow in the Sioux Basin was likely restricted to relatively thin and discontinous proximal fluvial facies that could have been diagenetic paleoaquifers, in contrast to the extensive paleoaquifers in the Athabasca Basin that promoted large-scale diagenetic reactions and alteration that led to the formation of unconformity-type uranium mineralization. In addition, the non-radiogenic isotopic composition of leachable Pb in the Sioux Basin sandstones indicates that the majority of the Pb is from a normal crustal source, inconsistent with mobilization of radiogenic Pb from a uranium-rich source, such as a uranium deposit. Although the Sioux Basin shares similar general characteristics to the Athabasca Basin, the results of this study suggest that it has a lower potential than the Athabasca Basin to host significant high-grade unconformity-type deposits.

Keywords: Paleoproterozoic basins; Sioux Basin; Ar/Ar; Uranium deposits; Mazatzal Orogeny; Pb isotopes

* Corresponding author. Tel.: +1 306 956 6280; fax: +1 306 956 6390.
E-mail address: hanly@geoladm.geol.queensu.ca (A.J. Hanly).

0301-9268/$ – see front matter © 2006 Elsevier B.V. All rights reserved.
doi:10.1016/j.precamres.2006.03.007

1. Introduction

The Paleoproterozoic Sioux Basin comprises a series of sub-basins in a west-trending belt in southeastern South Dakota, southwestern Minnesota, and the northwestern corner of Iowa (Fig. 1). Sedimentary rocks that make up the remnants of the Sioux Basin are dominantly well-cemented quartz arenites that have been weakly affected by regional subgreenschist grade metamorphism, resulting in a strongly indurated rock and thus is commonly referred to as the "Sioux Quartzite". Several other "Quartzites" (i.e. Baraboo, Barron, McClasin, Waterloo, and Flambeau; Fig. 2) in the southern Lake Superior region are also remnants of quartz-rich sedimentary basins and the correlative nature of these quartzites has been the subject of ongoing debate. Dott (1983) suggested that, although the Sioux, Baraboo, and Barron Quartzites share many similarities, they may not be strictly correlative and he grouped them into what is commonly referred to as the "Baraboo Interval Quartzites", spanning the time from 1450 to 1750 Ma. To avoid any ambiguities associated with the term "Baraboo Interval Quartzites" and for the sake of brevity, the Sioux, Baraboo, Barron, McClasin, Waterloo, and Flambeau quartzites in the southern Lake Superior region will be referred to, in this paper, as the Lake Superior Quartzites.

The purpose of this paper is to address two interrelated aspects: (1) the correlative nature of the Sioux Basin to other quartzite-bearing basins in the Lake Superior region and (2) the unconformity-related uranium mineralization potential of the Sioux Basin.

The youngest $^{207}Pb/^{206}Pb$ ages of detrital zircons from the Lake Superior Quartzites indicate a maximum age of ca. 1750 Ma for the quartzites and demonstrate that they are clearly post-Penokean in age (Holm et al., 1998; Medaris et al., 2003; Van Wyck and Norman, 2004). Ar/Ar and Rb/Sr ages from mica and hornblende in the crystalline basement rocks underlying the quartzites define a thermal front in northern Wisconsin that separates post-Penokean cooling ages of 1750–1700 Ma in the north from lower ages of ca. 1570–1630 Ma to the south (Holm et al., 1998; Romano et al., 2000; Fig. 2). The ca. 1.6 Ga ages are thought to reflect isotopic resetting due to low-grade metamorphism and deformation in response to the Mazatzal Orogeny and is likely contemporaneous with folding and deformation of the Baraboo, Flambeau, and Waterloo quartzites (Romano et al., 2000; Medaris et al., 2003). Holm et al. (1998) suggested that the lack of deformation of the Sioux and Barron quartzites may indicate that they are younger than the other aforementioned, deformed quartzites or are outside the region of post-Penokean deformation.

In this study, we obtained $^{40}Ar/^{39}Ar$ ages of ca. 1615–1465 Ma from muscovite in the Sioux Basin that likely reflect perturbation of the Ar systematics in muscovite in response to the 1.6 Ga Mazatzal Orogen and a later 1.5–1.4 Ga transcontinental (?) magmatic event. This provides the first direct evidence that the Sioux Basin has experienced a similar tectonic history to other quartzites in the Lake Superior region and indicates that the Sioux Basin is likely not younger than the more deformed quartzites, lending support to the hypothesis that these quartzites are indeed correlative.

The Sioux Basin is also similar in age and has similar lithological characteristics to the Paleoproterozoic Athabasca Basin in Canada, which is host to world-class unconformity-related uranium deposits. Both the Sioux and Athabasca basins are dominated by supermature

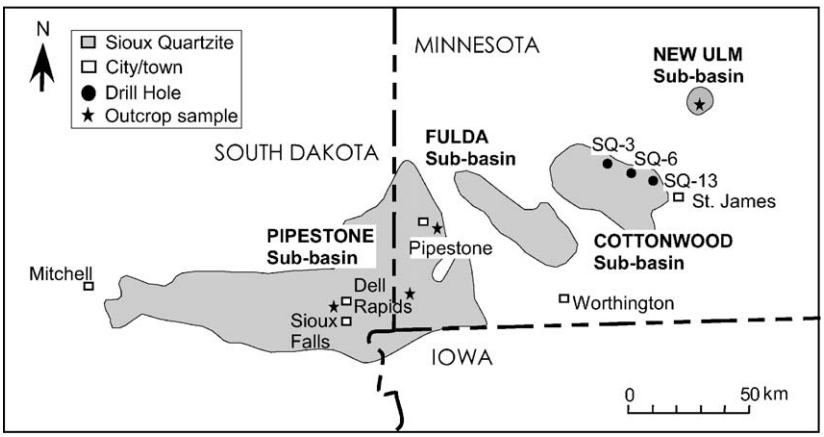

Fig. 1. Location map for the Sioux Basin showing the Pipestone, Cottonwood, Fulda, and New Ulm Sub-basins (modified from Southwick and Mossler, 1984). Also shown are the location of the three drill cores and outcrop samples that were examined in this study.

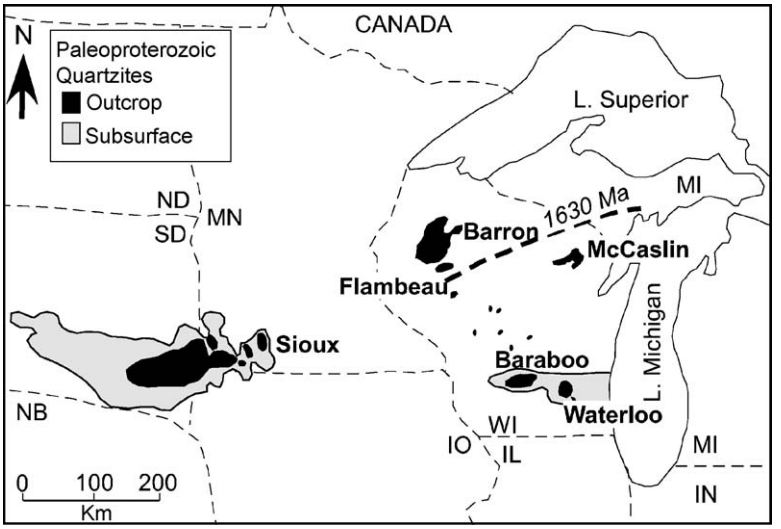

Fig. 2. Location map for Paleoproterozoic quartzites in northcentral USA: Sioux, Barron, Flambeau, McCaslin, Baraboo, and Waterloo quartzites (modified from Medaris et al., 2003). The dashed line represents the ca. 1630 Ma thermal and tectonic front in northern Wisconsin and southern Michigan based on $^{40}Ar/^{39}Ar$ cooling ages from basement minerals (Holm et al., 1998; Romano et al., 2000).

quartz arenite facies that are mainly fluvial in origin and were deposited in a warm, humid climate under oxidizing conditions (Ramaekers, 1981; Ojakangas and Weber, 1984; Southwick et al., 1986; Kotzer et al., 1992; Kotzer and Kyser, 1995). These general similarities have led to speculations that the Sioux Basin may have the potential to host large, high-grade unconformity-related uranium deposits similar to those in the Athabasca Basin (e.g. Ansfield and Stach, 1981; Southwick et al., 1982). There is a notable lack of research focusing on this important aspect of the Sioux Basin and, as such, this is one of the key objectives of this research.

Several models have been proposed for the generation of unconformity-related uranium deposits and these can be broadly categorized into three main hypotheses: (1) near-surface supergene (e.g. Knipping, 1974; Langford, 1974); (2) magmatic-hydrothermal or metamorphic-hydrothermal (e.g. Little, 1974; Morton, 1976; Munday, 1979) and (3) diagenetic-hydrothermal, which is the favored model among many researchers (e.g. Hoeve and Sibbald, 1978; Eye et al., 1983; Ruzicka, 1993; Hoeve and Quirt, 1984; Wilson et al., 1987; Wilde et al., 1989; Kotzer and Kyser, 1995; Raffensperger and Garven, 1995a,b; Sopuck and Wasyliuk, 1996; Kyser et al., 2000).

Proterozoic continental sedimentary basins are host to major unconformity-related uranium deposits and there are several factors that are common among such basins that have led to the diagenetic-hydrothermal model for unconformity-related deposits. First, there must be a uranium source and it is generally believed that uranium-rich minerals, such as zircon and apatite that are present in basin-filling siliciclastic sediments are leached during burial diagenesis by oxygen-bearing pore fluids (Hoeve and Sibbald, 1978; Hoeve et al., 1980; Hoeve and Quirt, 1984, 1987; Ruzicka, 1993; Kotzer and Kyser, 1995; Fayek and Kyser, 1997; Kyser et al., 2000). Mass-balance calculations have shown that uranium-rich detrital minerals in continental basins thousands of square kilometers in aerial extent, such as the Athabasca Basin, would easily provide enough uranium to produce the largest such deposits (Fayek and Kyser, 1997). Uranium can be mobilized in oxidized complexes, but is immobile in reducing ones. Pore fluid preferentially moves along unconformity surfaces and when the oxygenated uranium-bearing basinal fluids interact with reducing fluids emanating from fractures rooted in the crystalline basement, uranium is precipitated at this geochemical interface, at or near the unconformity (e.g. Fayek and Kyser, 1997; Kyser et al., 2000). An alternative model suggests that uranium is sourced from crystalline basement lithologies (e.g. Tremblay, 1982; Dahlkamp, 1978, 1993; Fogwill, 1985; Annesley et al., 1995, 1996; Wheatley et al., 1996). This model, however, suffers from a viable mobilization and precipitation mechanism.

The basin and its subsequent diagenetic evolution plays key roles in the formation of unconformity-related uranium mineralization, as shown by many studies of unconformity-related uranium deposits in the Paleoproterozoic Athabasca Basin in Canada and Kombolgie Sub-basin in Australia (e.g. Hoeve and Quirt, 1984, 1987; Wilde and Wall, 1987; Wilde et al., 1989; Kotzer

et al., 1992; Kotzer and Kyser, 1995; Raffensperger and Garven, 1995a,b; Kyser et al., 2000; Kyser and Hiatt, 2003; Polito et al., 2004). Because the basin itself plays such a central role in the development of Proterozoic uranium deposits, a holistic approach, involving the integration of data from sedimentology, stratigraphy, diagenesis and the geology of sedimentary basins, is necessary to understand paleohydrologic systems in terms of basin evolution (e.g. Kyser et al., 2000; Kyser and Hiatt, 2003; Hiatt et al., 2003).

A holistic approach was utilized here to determine the uranium mineralization potential of the Sioux Basin that specifically, included: (1) assessment of the characteristics of the depositional and diagenetic paleoaquifers based on field studies of sedimentological and stratigraphic relationships and thin-section scale studies of the paragenesis of diagenetic minerals; (2) stable isotope analysis and petrographic studies of diagenetic clay minerals to determine the origin and relative timing of diagenetic fluids; (3) $^{40}Ar/^{39}Ar$ dating of muscovite from the Sioux Basin to further constrain the timing of diagenesis and subsequent fluid events, especially those related to far-field tectonic events, such as the Mazatzal Orogeny and (4) determination of leachable Pb isotopic compositions to assess whether these compositions reflect Pb mobilized from a uranium-rich source such as an unconformity-related uranium deposit (e.g. Holk et al., 2003). The results from this approach are compared to those from the uranium-rich Athabasca Basin to assess the prospectivity of the Sioux Basin to host unconformity-related uranium deposits.

2. Geologic considerations

2.1. Geology of the Sioux Basin

The Sioux Basin is comprised of red, maroon and grey colored quartz arenites, basal conglomerates and thin muddy interbeds. Metamorphism of the basin was subgreenschist grade and faulting, gentle folding and subsequent erosion may have resulted in the development of the sub-basins (Ojakangas and Weber, 1984; Southwick and Mossler, 1984). Outcrops of the Sioux Basin are sparse, but subcrop is extensive beneath Cretaceous and Quaternary cover rocks. The lack of three-dimensional stratigraphic relationships and lateral continuity of outcrop exposure has hindered attempts to formally subdivide the basin fill into distinct lithostratigraphic units.

Basal conglomerates of the Sioux Basin unconformably overlie complex crystalline basement rocks of the Archean Minnesota River Valley Superior Subprovince and minor Paleoproterozoic intrusions, and a well-developed paleoregolith up to 20 m thick that occurs at the unconformity (Southwick and Mossler, 1984). The sub-Sioux Basin paleoregolith is characterized by intensive alteration of coarse-grained metamorphic feldspar to fine-grained muscovite and kaolinite, and introduction of secondary hematite and silica, which Southwick and Mossler (1984) indicate may be comparable to zones three and four of weathered bedrock as described by Ruxton and Berry (1957). The majority of the basin fill consists of supermature quartz arenites with an overall estimated thickness of 1–3 km (Baldwin, 1951). Stratigraphic and sedimentological evidence indicates that the majority of the quartz arenities were deposited in a distal braided river environment (Morey, 1984; Ojakangas and Weber, 1984; Southwick and Mossler, 1984; Southwick et al., 1986), although the upper part of the Sioux Basin contains sedimentary structures that may indicate a change from a fluvial environment to a tidally influenced, shallow marine environment (Ojakangas and Weber, 1984).

The age and extent of magmatic rocks associated with the Sioux Basin are poorly constrained. In northwestern Iowa, the Sioux Basin is reportedly intercalated with rhyolites that have an apparent Rb/Sr age of 1470 ± 50 Ma (Lidiak, 1971) and mafic intrusives of unknown age, associated with or intruding the Sioux Basin, have been reported near Sioux Falls and Corson, South Dakota (Goldich et al., 1961; Stach et al., 1981; Sklar, 1983).

2.2. Tectonic history/setting

The Lake Superior Quartzites in the north central United States and other Paleoproterozoic basins in North America (e.g. Athabasca and Thelon Basins in Canada) all record widespread continental sedimentation following the amalgamation at ca. 2.0–1.8 Ga ago of Archean microcontinents to form the bulk of Laurentia (Fig. 3). The 1870–1830 Ma Penokean orogeny (Sims et al., 1989) in the southern Lake Superior region represents an island-arc/back-arc and continent collision along the southern margin of the Superior Province, which has deformed and metamorphosed Archean and Paleoproterozoic rocks (Fig. 3). Renewed convergence on the southern margin of Laurentia is marked by a change in subduction direction from the south during the Penokean Orogeny to the north during the 1.8–1.7 Ga Yavapai Orogeny (Holm et al., 2005; Fig. 3). Subduction of the Yavapai plate resulted in magmatic pulses at ca. 1800, 1775 and 1750 Ma, becoming younger in a southeastward direction across the Penokean terrane, likely as a result of slab rollback (Holm et al., 2005). The slab rollback model proposed by Holm et al. (2005)

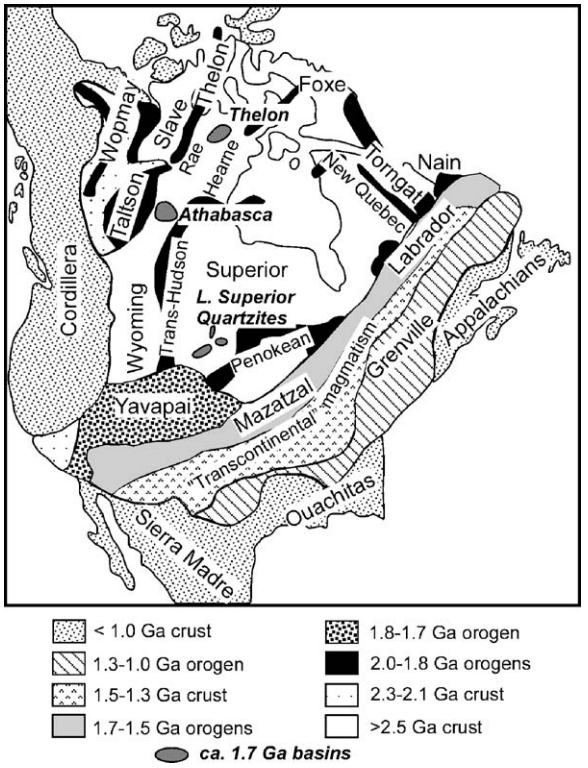

Fig. 3. Schematic tectonic map of North America showing the distribution of Proterozoic (2.0–1.0 Ga) crustal provinces and representative ca. 1.7 Ga basins that are part of Laurentia (modified from Hoffman, 1988, 1989; Karlstrom et al., 2001; Holm et al., 2005).

has important implications for the tectonic history of the Lake Superior Region. The model suggests that a combination of magma induced thermal weakening and a reduction of compressional stresses due to slab steepening of the Yavapai plate ultimately resulted in extensional collapse of overthickened portions of the Penokean crust; followed by a period of cratonic stability from ca. 1750 to 1650 Ma, during which the Lake Superior Quartzites were deposited. Following deposition of the Lake Superior Quartzites, a compressional tectonic regime resumed on the southern margin of Laurentia at ca. 1650–1630 Ma during the Mazatzal Orogeny (Holm et al., 1998; Romano et al., 2000; Medaris et al., 2003; Holm et al., 2005; Fig. 3). Ar/Ar and Rb/Sr ages from mica and hornblende in the basement rocks underlying the quartzites define a thermal front in northern Wisconsin that separates post-Penokean cooling ages of 1750–1700 Ma in the north from lower ages of ca. 1630 Ma to the south (Holm et al., 1998; Romano et al., 2000; Fig. 2). The ca. 1630 Ma ages are thought to reflect isotopic resetting due to low-grade metamorphism and deformation in response to the Mazatzal Orogeny and is likely contemporaneous with folding and deformation of some of the Lake Superior Quartzites (Romano et al., 2000; Medaris et al., 2003). It has been suggested by Holm et al. (2005) that preservation of the 1750–1700 Ma ages to the north is a reflection of strength differences in the crust, due to steepening of the subduction zone during post-Penokean magmatism related to the Yapavai Orogeny.

The broad-scale tectonic setting of the Sioux Basin and the Lake Superior Quartzites has been interpreted by Dott (1983) and Ojakangas and Weber (1984) as representative of deposition on a stable, passive continental margin based on the thickness of the quartzites and presence of marine rocks overlying the Baraboo Quartzite. Alternatively, Greenburg and Brown (1984) suggested that the Lake Superior Quartzites formed in response to anorogenic uplift following the Penokean Orogeny and Southwick and Mossler (1984) added that clasts of anorogenic rhyolite and tuff in conglomerates from the Pipestone Sub-basin point to a cratonic origin. More recently, Holm et al. (2005) suggested that deposition of the quartzites should be considered in the context of a continuous plate-margin tectonic setting, with exhumation and uplift of Penokean Orogenic rocks due to crustal weakening and subduction-related magmatism during the ca. 1800–1750 Ma Yavapai Orogeny, followed by a period of cratonic stability and deposition of the Lake Superior Quartzites from ca. 1750 to 1650 Ma, and renewed convergence at ca. 1.6 Ga during the Mazatzal Orogeny.

3. Analytical techniques and methodology

Ninety polished thin-sections from the Sioux Basin were examined by transmitted and reflected light microscopy and scanning electron microscopy (SEM) to determine the mineralogy, texture, and paragenetic sequence of mineral deposition. A portable infrared mineral analyzer (PIMA) was used to determine the clay minerals present in each sample and to aid in the selection of appropriate samples for clay mineral separation. Clay minerals for isotopic analyses and $^{40}Ar/^{39}Ar$ dating were separated from crushed rock samples using ultrasonic dispersion and centrifuge techniques and analyzed by XRD to determine the proportion of clay mineral phases using the method described by Mellinger (1979). Muscovite crystallinity was determined using the method of Kubler (1964, 1968) and is reported as the Kubler Index (KI). $^{40}Ar/^{39}Ar$ dating of muscovite was undertaken at Queen's University Ar-Geochronology Laboratory using the laser step-heating technique of Lee et al. (1990).

Oxygen in minerals was extracted using the conventional BrF_5 technique of Clayton and Mayeda (1963) and hydrogen from minerals was extracted online using a Thermo Finnigan thermo-combustion elemental analyzer (TC/EA) using a modified procedure of Sharp et al. (2001). The conventionally extracted gases were analyzed on a Finnigan MAT 252 mass spectrometer and online extractions by a Thermo Finnigan DELTAplusXP IRMS at the Queen's Facility for Isotope Research (QFIR). The isotopic compositions are reported using delta (δ) notation in units of per mil (‰) relative to Vienna Standard Mean Ocean Water (V-SMOW). Reproducibility of $\delta^{18}O$ measurements based on repeat measurements of reference materials is ±0.2‰, and for δD is ±5‰. The oxygen isotopic composition of the fluids in equilibrium with the minerals was calculated from the isotope fractionation factors of O'Neil and Taylor (1969) for muscovite-water and Land and Dutton (1978) for kaolinite-water. For hydrogen, illite-water of Yeh (1980) and kaolinite-water of Gilg and Sheppard (1996) fractionation factors were used. The fractionation factor for illite-water was used instead of muscovite-water for calculating δD fluid values because an appropriate hydrogen fractionation factor for muscovite-water at temperatures lower than 400 °C is not available.

Nineteen drill core and outcrop samples from the Sioux Basin were analyzed for their Pb isotopic ratios and trace element concentrations using a Finnigan MAT Element™ high-resolution ICP-MS at QFIR. The samples were prepared and analyzed using a weak 2% nitric acid partial leach as described by Holk et al. (2003).

4. Results

4.1. Paleoaquifer characteristics and petrogenesis of the Sioux Basin

Three drill cores from the Cottonwood Sub-basin were examined to determine lithostratigraphic and paleoaquifer characteristics of sedimentary facies (Fig. 4). In the basal part of the Cottonwood Sub-basin, coarse-grained sandstones and conglomerates that were

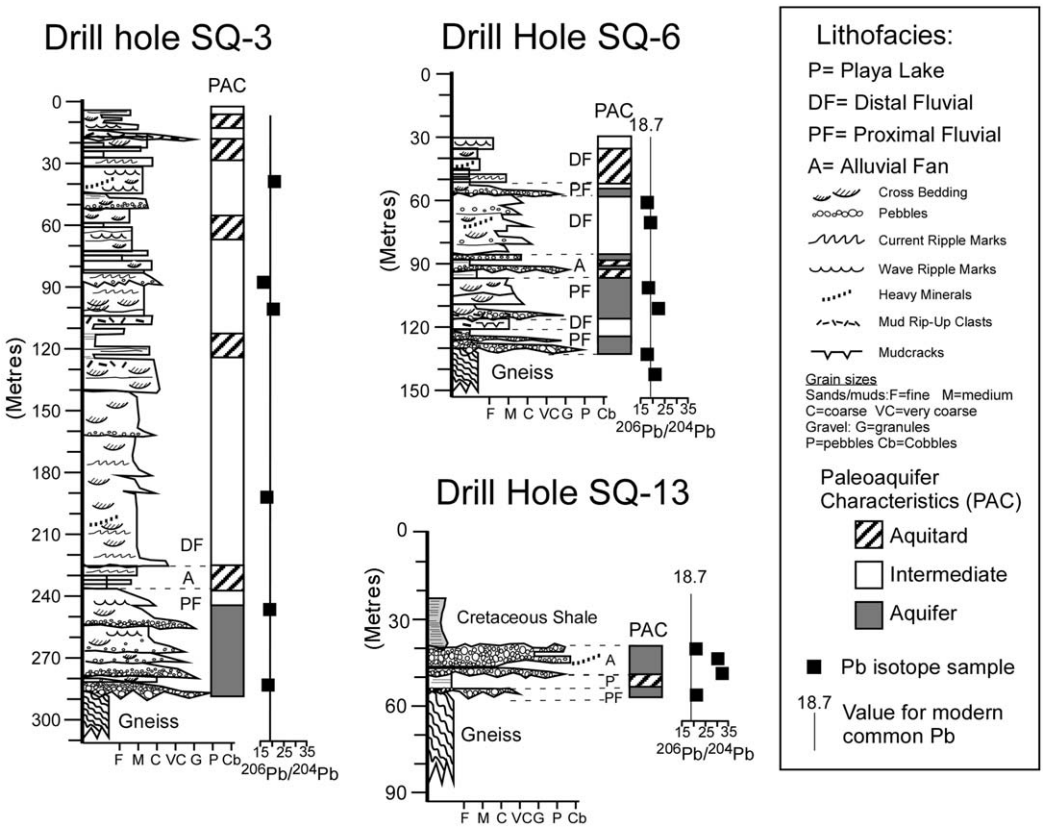

Fig. 4. Stratigraphic sections showing the vertical succession of lithofacies and diagenetic paleoaquifer characteristics of three drill cores in the Cottonwood Sub-basin (location of drill holes are shown in Fig. 1) and $^{206}Pb/^{204}Pb$ ratios of leachable Pb extracted with 2% HNO_3 from sandstones of the Sioux Basin. The solid line represents the $^{206}Pb/^{204}Pb$ ratio of 18.7 for modern common Pb (Stacey and Kramers, 1975).

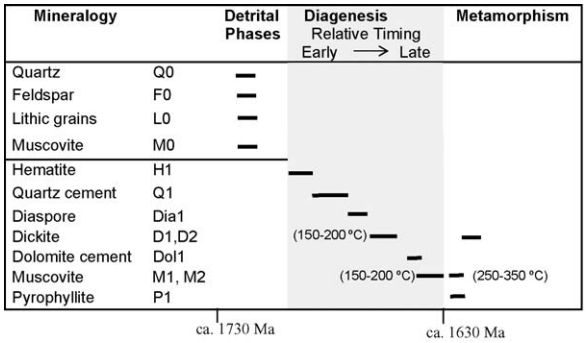

Fig. 5. Paragenetic sequence of minerals for the Sioux Basin. Temperatures of diagenesis and metamorphism are based on kaolin group polytype (i.e. dickite) and muscovite crystallinities. Timing of diagenesis is constrained by the maximum age of the Sioux Basin reported by Holm et al. (1998) and age of regional metamorphism based on Rb/Sr and Ar/Ar ages for minerals from deformed regional basement rocks (Holm et al., 1998; Romano et al., 2000) and Ar/Ar ages of muscovite from the Sioux Basin in this study.

deposited in proximal braided streams and alluvial fans were likely excellent paleoaquifers during diagenesis (i.e. diagenetic paleoaquifers; Fig. 4). In comparison, finer-grained, well-sorted sandstones deposited in a distal fluvial environment, were likely good paleoaquifers during deposition but were cemented early during burial diagenesis (i.e. diagenetic aquitards or intermediate diagenetic paleoaquifers; Fig. 4). Thin, muddy units deposited in distal alluvial fan and playa lake environments were depositional and diagenetic aquitards that punctuated and segmented the diagenetic paleoaquifers (Fig. 4).

The Sioux Basin is mainly comprised of fine-medium grained, well-sorted quartz arenites and detailed studies of thin-sections have enabled a mineral paragenesis to be determined for the Sioux Basin (Fig. 5). The main detrital component, typically 95% of the mode of the sandstones, is subrounded to rounded quartz (Q0). Diagenetic minerals consist of syntaxial quartz overgrowths (Q1; Fig. 6a) and less commonly, later diaspore (Dia1) and rare dolomite (dol1) cement. Diaspore (Dia1) commonly occurs as large poikiolotopic crystals (Fig. 6b) enclosing quartz grains and typically has been altered to dickite (D1; Fig. 6b) and more rarely, pyrophyllite (P1; Fig. 6b).

Minor detrital components in the Sioux Basin include lithic grains (L0) and feldspars (F0) that typically make up <1% of the total volume of the sandstones and are commonly replaced by dickite (D1) filling pore spaces or as pseudomatrix (Fig. 6c and d). PIMA analysis indicates that the majority (>90%) of the kaolin type clay minerals in the sandstones are not kaolinite, but the higher temperature polymorph, dickite. Muscovite (M1) that formed during peak burial diagenesis occurs as a replacement of diagenetic dickite (D1) and in pore spaces (Fig. 6d and e). Trace amounts of detrital tourmaline, muscovite, rounded zircon, and Fe/Ti oxides occur mainly in heavy mineral laminations, particularly in well-sorted, quartz-cemented units that are distal fluvial facies (e.g. Fig. 4).

Regional metamorphism of the Sioux Basin produced minor amounts of pyrophyllite (P1), prograde muscovite (M2), and retrograde dickite (D2). That some of the muscovite in the Sioux Basin is likely the result of prograde metamorphism of earlier diagenetic muscovite (M1) is based on paragenetic relationships, crystallinity (Fig. 7) and $^{40}Ar/^{39}Ar$ ages (Section 4.3). Pyrophyllite (P1) formed as a prograde metamorphic replacement of dickite (D1), likely during the reaction dickite + 4 quartz = pyrophyllite + $2H_2O$, and more rarely, replaces diaspore (Dia1) according to the reaction: diaspore + 8 quartz = pyrophyllite. A second generation of dickite (D2) is coarser and commonly has a fibrous habit in comparison to finer-grained blocky early diagenetic dickite (D1), and occurs as a replacement of diaspore (Dia1; Fig. 6f) and a recrystallization product of earlier dickite (D1).

Table 1
$\delta^{18}O$ and δD values for dickite (D1) and muscovite (M1, M2) from the Cottonwood Sub-basin

Drill core ID	Depth (m)	Mineral	$\delta^{18}O_{mineral}$ (‰)	$\delta D_{mineral}$ (‰)	$\delta^{18}O_{fluid}$ ‰ (150 °C)	δD_{fluid} ‰ (150 °C)	$\delta^{18}O_{fluid}$ ‰ (200 °C)	δD_{fluid} ‰ (200 °C)
SQ-3	67.0	D1	9.6	−50	−1.5	−30	0.7	−33
SQ-3	73.0	D1	9.2	−46	−1.9	−26	0.3	−28
SQ-3	86.9	M1	11.9	−52	2.5	−32	5.2	−36
SQ-3	180.0	D1	9.2	−52	−1.9	−32	0.3	−34
SQ-6	82.9	D1	10.1	−50	−1.0	−30	1.2	−32
SQ-6	132.0	M1, M2	8.9	−60	−0.5	−40	2.2	−44
SQ-13	44.9	M1, M2	9.3	−62	−0.1	−42	2.6	−46

The $\delta^{18}O$ and δD fluid values were calculated at 150 to 200 °C. Refer to Fig. 1 for drill core locations.

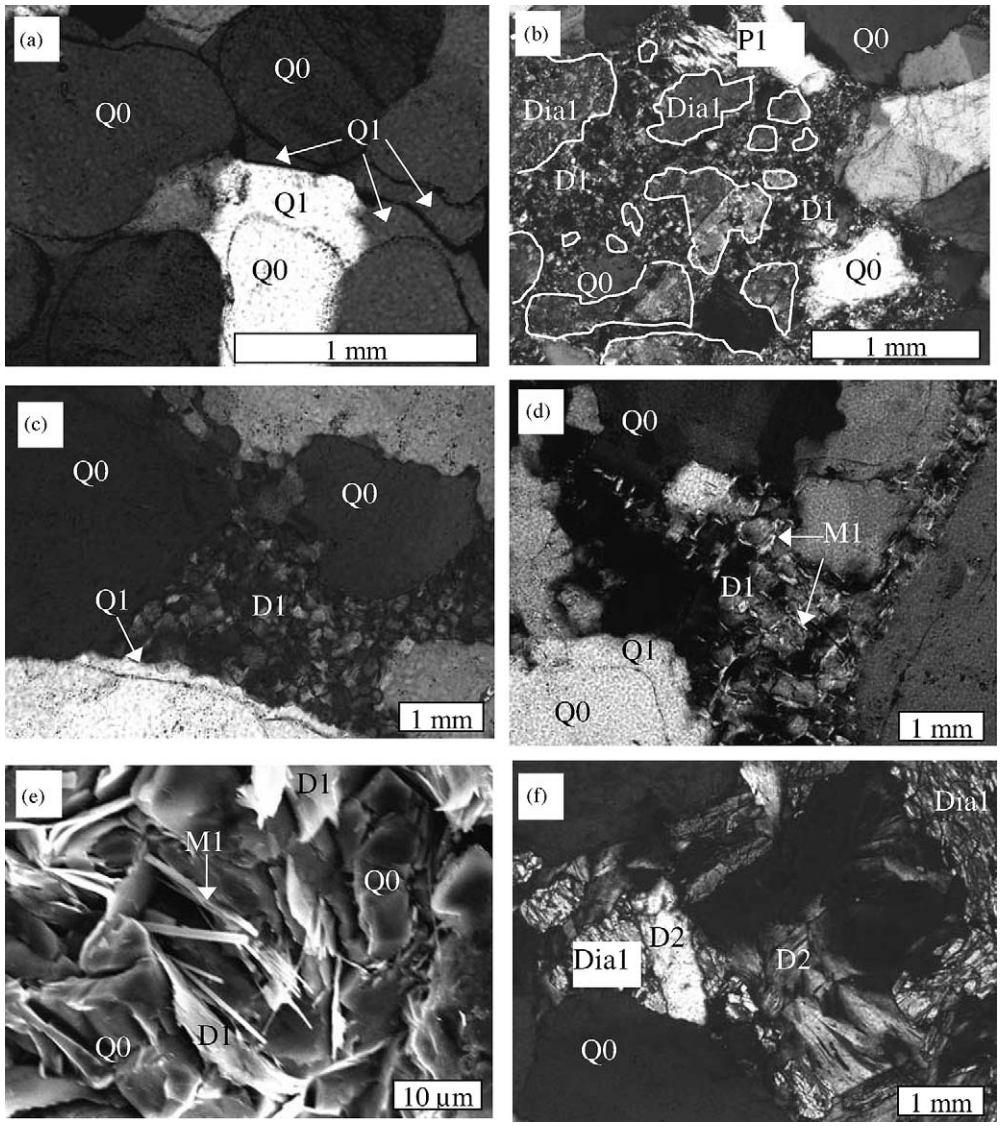

Fig. 6. (a) Photomicrograph in cross-polarized light of detrital quartz (Q0) and syntaxial quartz cement (Q1), sample SQ-DR1. (b) Photomicrograph in cross-polarized light of poikiolotopic crystals of diaspore (Dia1) outlined in white, replaced by early diagenetic dickite (D1) and prograde metamorphic pyrophyllite (P1), sample SQ-3-288. (c) Photomicrograph in cross-polarized light of early diagenetic dickite (D1) filling a pore space, sample SQ-6-354. (d) Photomicrograph in cross-polarized light of pseudomatrix comprised of early diagenetic dickite (D1) and showing replacement by fine-grained peak diagenetic muscovite (M1), sample SQ-6-132. (e) SEM secondary electron image of peak diagenetic muscovite (M1) in pore spaces, sample SQ-6-138. (f) Photomicrograph in cross-polarized light of coarse, fibrous retrograde dickite (D2) replacing diaspore (Dia1), sample SQ-3-190.

4.2. Hydrogen and oxygen compositions of basin fluids

To determine the isotopic composition of the pore fluids that were present during diagenesis in the Sioux Basin, we measured the hydrogen and oxygen isotopic compositions of early diagenetic dickite, D1, and diagenetic and metamorphic muscovite, M1 and M2 (Table 1). Both M1 and M2 were analyzed because muscovite is relatively scarce in the Sioux Basin and based on petrographic textures, crystallinity, and $^{40}Ar/^{39}Ar$ ages, metamorphic muscovite (M2) is likely a product of prograde regional greenschist metamorphism of diagenetic muscovite (M1). Therefore, the isotopic composition of metamorphic muscovite (M2) should reflect the isotopic composition of the precursor diagenetic muscovite (M1) because re-equilibration of original isotopic compositions of the parent rock during metamorphism is

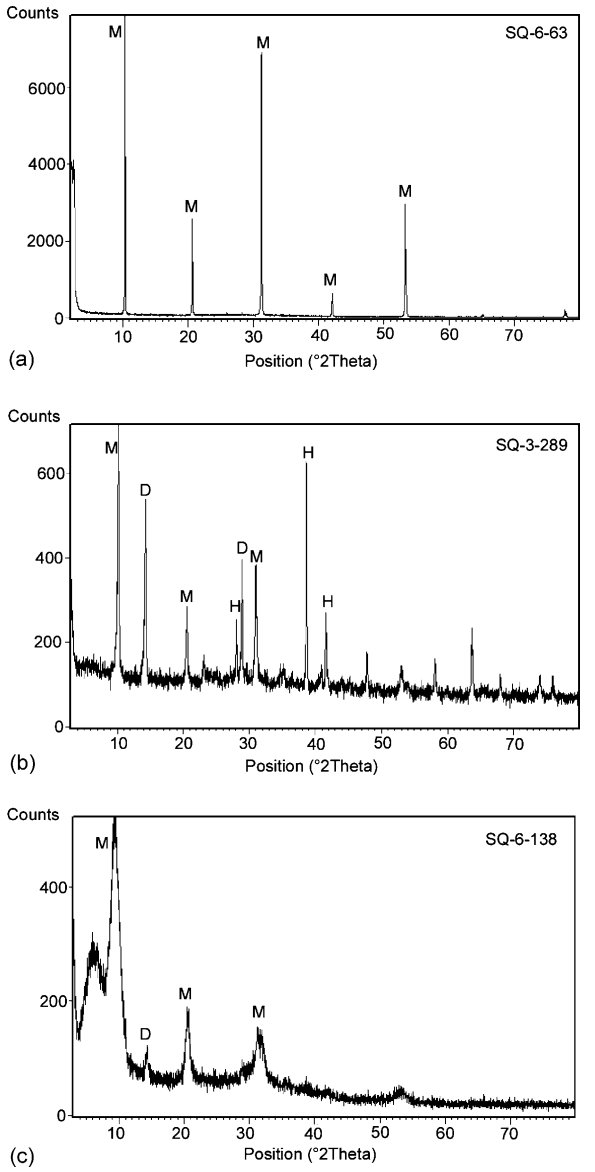

Fig. 7. Representative XRD spectra of muscovite from the Sioux Basin showing the variability in crystallinities based on the Kubler Index (Kubler, 1964, 1968). (a) Sample SQ-6-63.0, Kubler Index = 0.1. (b) Sample SQ-3-289, Kubler Index = 0.3. (c) Sample SQ-6-138, Kubler Index = 1.0. Major peaks are labelled: M, muscovite; D, dickite; H, hematite.

generally insignificant at low metamorphic grades (e.g. Taylor, 1997) and also in the absence of large volumes of fluids at any metamorphic grade (e.g. Eiler and Valley, 1994; Taylor, 1997).

To calculate the $\delta^{18}O$ and δD values of the fluids in equilibrium with dickite and muscovite requires an estimate of their temperatures of formation. Dickite is the higher temperature polymorph of kaolinite and generally forms at temperatures of 150–250 °C as a result of hydrothermal alteration or medium–high-grade diagenesis (e.g. Ehrenberg et al., 1993; Zotov et al., 1998). Paragenetic relationships (Fig. 5) indicate that dickite (D1) formed earlier than diagenetic muscovite (M1), which has crystallinities that suggest formation temperatures of 150–200 °C (KI = 0.4–1.1). Therefore, the best estimate for crystallization temperatures for both early diagenetic dickite (D1) and diagenetic muscovite (M1) is 150–200 °C.

Assuming that 150–200 °C is a reasonable estimate of crystallization temperatures, the $\delta^{18}O$ and δD values of the fluids that formed in equilibrium with early diagenetic dickite (D1) are −1.9 to +1.2‰ and −26 to −34‰, respectively, and the fluids in equilibrium with peak diagenetic muscovite (M1) have $\delta^{18}O$ and δD values of −0.5 to +5.2‰ and −32 to −46‰, respectively (Fig. 8; Table 1). Some studies have demonstrated, that under certain circumstances, hydrogen in clay minerals can re-equilibrate with present day meteoric waters (e.g. Longstaffe and Ayalon, 1990; Kotzer and Kyser, 1995). This is not the case for clay minerals from the Sioux Basin, as the δD values for both dickite and muscovite are higher than would be expected if these minerals had isotopically re-equilibrated with recent meteoric waters, which have present day δD compositions that range from −60 to −80‰ (Kendall and Coplen, 2001). In addition, hydrogen isotope exchange of ancient clay minerals with more recent meteoric waters is commonly associated with high water/rock ratios, which is not evident in

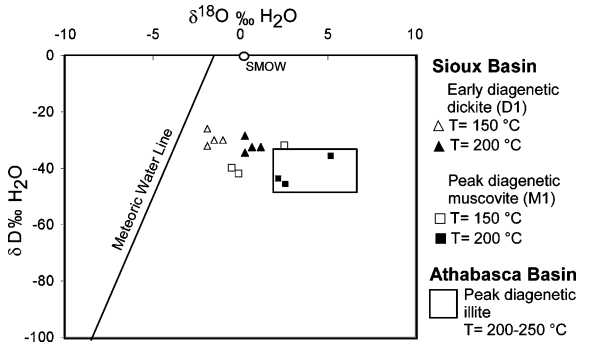

Fig. 8. $\delta^{18}O$ and δD values for fluids in the Sioux Basin in equilibrium with peak diagenetic muscovite (M1) and early diagenetic dickite (D1) at 150 and 200 °C. Shown for comparison are the isotopic compositions of fluids associated with peak diagenesis and unconformity-type uranium mineralization in the Athabasca Basin (Kotzer and Kyser, 1995) and the meteoric water line, which represents the isotopic compositions of global meteoric waters (Craig, 1961). Note that fluids associated with peak diagenetic muscovite in the Sioux Basin have similar characteristics as peak diagenetic illite from the Athabasca Basin. Abbreviations: SMOW, Standard Mean Ocean Water.

the Sioux Basin. Therefore, the δD_{fluid} values for both dickite (D1) and muscovite (M1) most likely reflect the composition of the fluids from which they formed and indicate that the main sources were meteoric paleofluids with a possible small contribution from evaporated seawater. The low and narrow range of $\delta^{18}O_{fluid}$ values for dickite (D1) indicate limited interaction of the pore fluids with the host rocks during early diagenesis, whereas muscovite (M1) has higher $\delta^{18}O_{fluid}$ values consistent with more evolved fluids during peak diagenesis (Fig. 8).

4.3. $^{40}Ar/^{39}Ar$ dating of muscovite

The $^{40}Ar/^{39}Ar$ incremental step heating method has distinct advantages over other methods of dating sedimentary rocks, such as K-Ar and total fusion $^{40}Ar/^{39}Ar$, with perhaps the most notable advantage being the determination of meaningful ages from discordant age spectrum (Dallmeyer, 1979; Hanes, 1991). In the step heating method, the results of the experiment are commonly plotted as the apparent age of the gas fraction analyzed versus the fraction of ^{39}Ar released as the temperature is increased with the resulting plot referred to as an age spectrum (e.g. Fig. 9). This technique can be used to reveal the different sources of Ar within a sample and elucidate the conditions under which partial Ar loss can occur (e.g. thermal overprinting), as first documented by Merrihue and Turner (1966).

Seven samples of muscovite were extracted from drill core samples in the Sioux Basin and underlying basement rocks for $^{40}Ar/^{39}Ar$ laser step heating analysis at QFIR (Table 2; Fig. 9). As the Ar spectra are commonly disturbed, the majority of the ages are reported as pseudoplateau ages, which for the purpose of this study are defined as the maximum apparent $^{40}Ar/^{39}Ar$ age recorded in one or more successive heating steps but represent <50% of the total ^{39}Ar released. A more strict definition is applied to reporting plateau ages, which is that part of the age spectrum diagram composed of contiguous gas fractions that represent >50% ^{39}Ar released and for which there is no discernable age difference between any two gas fractions at the 95% confidence level (e.g. Fleck et al., 1977).

Detrital muscovite (M0) from sample SQ-6-137, which is from gneissic basement rocks just below the sub-Sioux Basin basal unconformity, has a plateau age of 1831 ± 11 Ma. This age corresponds with deformation and metamorphism of the basement rocks during the Penokean Orogeny from 1870 to 1830 Ma (Sims et al., 1989). A few metres above the unconformity in the sandstones, detrital muscovite (M0) from sample SQ-6-128 has a disturbed Ar spectrum with a pseudoplateau

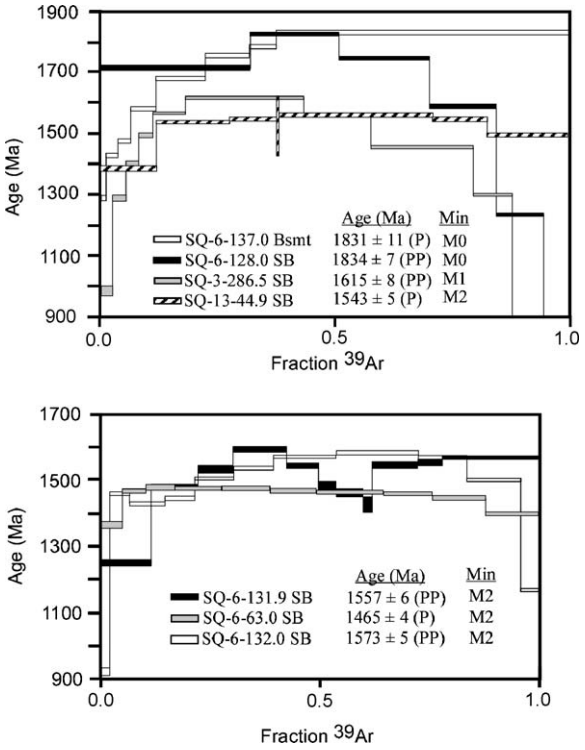

Fig. 9. $^{40}Ar/^{39}Ar$ spectra and ages for muscovite from the Sioux Basin and underlying basement rocks. Abbreviations: Bsmt, basement; SB, Sioux Basin; P, plateau age; PP, pseudoplateau age; Min, mineral analyzed; M0, detrital muscovite; M1, diagenetic muscovite; M2, metamorphic muscovite.

age of 1834 ± 7 Ma, indicating that the source of the detrital muscovite is likely from the underlying basement rocks and that the Ar systematics in muscovite were not completely reset during diagenesis. Some perturbation of the Ar in this sample during diagenesis may be indicated by the lowest temperature step that has an apparent $^{40}Ar/^{39}Ar$ age of 1724 ± 7 Ma (Fig. 9). This gas fraction represents Ar contained within grain margins that is more prone to isotopic resetting and therefore may provide an upper limit to the time of disturbance of the Ar system (e.g. Hanes, 1991).

A ca. 1615 Ma pseudoplateau age is recorded in diagenetic muscovite (M1) from sample SQ-3-286.5, that is close to the unconformity, and has a Kubler Index of 0.4 corresponding to an estimated temperature of crystallization of 200 °C. The relatively low temperature of crystallization (i.e. lower than the Ar closure temperature of muscovite) indicates that the $^{40}Ar/^{39}Ar$ age probably reflects isotopic resetting due to fluid migration as a result of a far-field tectonic event, such as the ca. 1.6 Ga Mazatzal Orogeny. In comparison, lower plateau and pseudoplateau $^{40}Ar/^{39}Ar$ ages of 1573–1465 Ma are

Table 2
Individual step-heating ages (Ma ± 2σ), argon isotope ratios, Ca/K ratios, % ^{40}Ar atmospheric contents, and % ^{39}Ar released for muscovite from the Sioux Basin and underlying basement rocks

Step	^{36}Ar/^{40}Ar	^{39}Ar/^{40}Ar	Ca/K	^{40}Ar (atm %)	^{39}Ar (%)	^{40}Ar*/^{39}Ar$_{K}$	Age (Ma)
SQ-6-137.0 < 2 μm, KI: 1.1 Mineral = M0, Plateau age: 1831 ± 11 Ma (62.6% ^{39}Ar)							
1	0.000159	0.026	0.049	4.70	1.21	36.33	1289 ± 10
2	0.000122	0.023	0.050	3.60	2.44	42.04	1428 ± 6
3	0.000128	0.022	0.055	3.78	2.62	44.08	1475 ± 8
4	0.000088	0.020	0.055	2.60	5.44	48.85	1581 ± 7
5	0.000078	0.018	0.062	2.31	10.54	53.57	1680 ± 7
6	0.000057	0.017	0.074	1.68	9.47	57.23	1753 ± 7
7	0.000064	0.017	0.049	1.89	5.72	58.80	1784 ± 8
8	0.000048	0.016	0.067	1.42	62.56	61.26	1831 ± 7
SQ-3-286.5 > 5 μm, KI: 0.4 Mineral = M0, Psuedoplateau age: 1615 ± 8 Ma							
1	0.001572	0.021	0.097	46.37	2.88	25.24	984 ± 17
2	0.000482	0.024	0.094	14.22	2.91	36.19	1286 ± 10
3	0.000211	0.023	0.057	6.22	2.72	40.78	1399 ± 9
4	0.000121	0.022	0.054	3.56	3.10	44.76	1492 ± 8
5	0.000067	0.020	0.071	1.97	6.82	47.97	1563 ± 6
6	0.000014	0.020	0.050	0.40	25.19	50.37	1615 ± 6
7	0.000012	0.021	0.048	0.34	14.15	47.67	1557 ± 6
8	0.000009	0.023	0.063	0.25	21.84	43.09	1453 ± 6
9	0.000013	0.027	0.087	0.38	8.47	36.67	1298 ± 5
10	0.000078	0.043	0.154	2.29	11.93	22.48	899 ± 4
SQ-6-132.0 2–5 μm, KI: 0.3 Mineral = M1, Pseudoplateau age: 1573 ± 5 Ma							
1	0.000634	0.036	0.039	18.70	1.88	22.89	924 ± 12
2	0.000255	0.022	0.032	7.52	4.69	42.58	1458 ± 7
3	0.000100	0.024	0.033	2.95	7.88	41.30	1428 ± 6
4	0.000044	0.024	0.026	1.29	6.75	41.99	1444 ± 6
5	0.000020	0.022	0.023	0.60	8.98	44.58	1505 ± 6
6	0.000021	0.022	0.018	0.61	9.17	45.89	1534 ± 6
7	0.000003	0.021	0.018	0.09	14.34	47.45	1569 ± 6
8	0.000016	0.021	0.017	0.48	18.73	48.07	1583 ± 6
9	0.000011	0.021	0.017	0.31	11.09	47.21	1564 ± 6
10	0.000004	0.023	0.121	0.12	12.48	44.34	1499 ± 5
11	0.000014	0.032	0.038	0.40	4.02	31.26	1171 ± 5
SQ-6-128.0 2–5 μm, KI: 0.6 Mineral = M2, Pseudoplateau age: 1834 ± 7 Ma							
1	0.000087	0.018	0.0270	2.57	31.68	54.80	1724 ± 7
2	0.000023	0.016	0.0220	0.67	18.77	60.37	1834 ± 7
3	0.000022	0.018	0.0250	0.65	19.35	56.40	1756 ± 6
4	0.000003	0.020	0.0200	0.10	14.07	48.80	1599 ± 6
5	0.000006	0.029	0.0310	0.19	10.07	33.95	1243 ± 6
6	0.000080	0.123	0.0590	2.35	6.05	7.93	376 ± 5
SQ-6-131.9 2–5 μm, KI: 0.3 Mineral = M2, Pseudoplateau age: 1557 ± 6 Ma							
1	0.000158	0.019	0.077	4.66	11.85	50.97	1250 ± 8
2	0.000035	0.015	0.062	1.02	10.58	64.63	1477 ± 9
3	0.000026	0.015	0.036	0.76	7.93	68.09	1530 ± 11
4	0.000021	0.014	0.039	0.63	12.17	72.10	1590 ± 8
5	0.000037	0.014	0.039	1.11	7.39	68.76	1540 ± 10
6	0.000015	00015	0.035	0.44	4.00	64.74	1479 ± 15
7	0.000031	0.016	00031	0.93	5.99	63.50	1460 ± 12
8	0.000049	0.016	0.055	1.44	2.29	61.29	1424 ± 23
9	0.000022	0.014	0.033	0.64	10.22	68.94	1543 ± 10
10	0.000006	0.014	0.040	0.18	5.57	69.36	1550 ± 12
11	0.000002	0.014	0.024	0.06	22.01	70.42	1565 ± 7

Table 2 (*Continued*)

Step	$^{36}Ar/^{40}Ar$	$^{39}Ar/^{40}Ar$	Ca/K	^{40}Ar (atm %)	^{39}Ar (%)	$^{40}Ar^{*}/^{39}Ar_{K}$	Age (Ma)
SQ-6-63.0 2–5 μm, KI: 0.3 Mineral = M2, Plateau age: 1465 ± 4 Ma (70.8% ^{39}Ar)							
1	0.000253	0.016	0.042	7.45	5.16	57.48	1362 ± 11
2	0.000031	0.016	0.036	0.90	5.39	63.72	1463 ± 8
3	0.000015	0.015	0.028	0.45	6.57	64.49	1475 ± 8
4	0.000018	0.015	0.028	0.54	10.89	64.20	1471 ± 7
5	0.000008	0.015	0.015	0.22	11.11	64.24	1471 ± 7
6	0.000007	0.015	0.018	0.22	10.65	63.74	1463 ± 8
7	0.000001	0.015	0.020	0.04	15.15	63.54	1460 ± 6
8	0.000004	0.015	0.023	0.11	11.08	63.25	1456 ± 6
9	0.000002	0.015	0.015	0.07	11.99	62.46	1443 ± 6
10	0.000005	0.015	0.036	0.16	11.92	59.46	1395 ± 6
11	0.000000	0.015	0.000	0.01	0.08	32.83	897 ± 440
SQ-13-44.9 2–5 μm, KI: 0.16 Mineral = M2, Plateau age: 1543 ± 5 Ma (70.4% ^{39}Ar)							
1	0.000090	0.017	0.041	2.64	12.22	58.36	1376 ± 7
2	0.000023	0.015	0.035	0.69	15.80	68.13	1530 ± 7
3	0.000008	0.015	0.032	0.24	10.06	68.80	1540 ± 9
4	0.000000	0.015	0.000	0.00	0.37	67.15	1515 ± 99
5	0.000004	0.014	0.031	0.12	32.76	69.63	1553 ± 7
6	0.000014	0.015	0.022	0.42	11.78	68.42	1535 ± 7
7	0.000005	0.015	0.031	0.14	16.53	65.35	1488 ± 7
8	0.000473	0.060	0.187	13.93	0.46	14.31	446 ± 130

Size fraction analyzed and muscovite crystallinity (KI = Kubler Index; Kubler, 1964, 1968) is also indicated. Abbreviations: $^{40}Ar^{*}$, radiogenic argon; $^{39}Ar_{K}$, argon from potassium during sample irradiation; M0, detrital muscovite; M1, diagenetic muscovite, M2, metamorphic muscovite.

recorded in metamorphic muscovite (M2) with Kubler Indexes of 0.16–0.3, corresponding to higher temperatures of 250–350 °C, consistent with resetting by a thermal event. The age spectra for muscovite (M2) from the Sioux Basin are complex (Fig. 9), so one interpretation is that the $^{40}Ar/^{39}Ar$ ages obtained from these samples record multiple events and therefore, represent mixing ages. Alternatively, deformation and metamorphism related to the Mazatzal Orogeny may have occurred over a prolonged period of time. This latter interpretation is supported by the range of ages of 1630–1579 Ma and 1614–1576 Ma reported by Holm et al. (1998) and Romano et al. (2000), respectively, for thermal resetting related to the Mazatzal Orogeny in the basement rocks beneath the deformed quartzites in Wisconsin. These ages are similar to plateau and pseudoplateau ages that range from 1615 to 1543 Ma for muscovite (M1 and M2) from the Sioux Basin. While the youngest plateau age of ca. 1465 Ma obtained from one muscovite sample from the Sioux Basin likely records the time of felsic magmatism in the region, as Lidiak (1971) reports 1470 ± 50 Ma rhyolites are intercalated with Sioux Basin quartz arenites in Iowa. Regardless of the interpretation, the range in $^{40}Ar/^{39}Ar$ ages of ca. 1615–1465 Ma recorded in muscovite (M1 and M2) from the Sioux Basin indicates a combination of both fluid and thermal resetting of the Ar systematics within muscovite occurred as a result of low-grade metamorphism related to the ca. 1.6 Ga Mazatzal Orogeny and later felsic magmatism at ca. 1450 Ma.

4.4. Pb isotope studies

Holk et al. (2003) provided the first comprehensive examination of the utility of using the compositions of leachable Pb in sandstones as an exploration tool for uranium mineralization in sedimentary basins. This technique is based on the principle that in situ radioactive decay of uranium minerals produces radiogenic Pb that can be mobilized away from the primary source by fluids and therefore, the composition of leachable Pb from sandstones can be used to determine the presence of a uranium-rich source. Furthermore, that radiogenic Pb loss actually occurs in uranium deposits is supported by numerous studies that report discordant U/Pb ages for uranium mineralization in major unconformity-related deposits in both Australia and Canada (e.g. Hills and Richards, 1976; Ludwig et al., 1987; Kotzer and Kyser, 1993; Fayek and Kyser, 1997; Polito et al., 2004).

Nineteen samples from three drill holes in the Cottonwood Sub-basin and outcrops at Blue Mound and New Ulm in the Sioux Basin were analyzed by HR-ICP-MS for their Pb isotopic compositions and total uranium and thorium contents (Table 3). For the purpose of this study, the most useful ratio is $^{206}Pb/^{204}Pb$ and values greater

Table 3
Summary of isotopic composition of Pb and total uranium and thorium leached with 2% HNO_3 for samples from the Sioux Basin

Sample	Depth (m)	$^{206}Pb/^{204}Pb$	$^{207}Pb/^{204}Pb$	$^{208}Pb/^{204}Pb$	$^{207}Pb/^{206}Pb$	Uranium (ppm)	Thorium (ppm)
SQ-3	40	20.27	16.36	41.77	0.81	0.086	0.112
SQ-3	88.7	17.88	15.81	38.44	0.88	b.d.	0.089
SQ-3	100	19.42	16.00	39.68	0.82	0.003	0.103
SQ-3	195	18.55	15.88	38.69	0.86	0.096	0.007
SQ-3	248	18.73	15.91	39.27	0.85	0.012	0.141
SQ-3	288	18.52	15.89	39.35	0.86	0.004	0.107
SQ-6	63	18.10	16.03	38.94	0.89	0.002	0.107
SQ-6	72.2	18.73	16.07	39.22	0.86	0.000	0.098
SQ-6	100	18.59	16.06	39.17	0.86	0.002	0.082
SQ-6	114	20.96	16.28	41.92	0.78	0.041	0.109
SQ-6	132	18.24	15.58	38.03	0.85	0.089	0.108
SQ-6	144	19.87	16.14	40.11	0.81	0.042	0.120
SQ-13	38	19.31	16.01	40.21	0.83	0.813	13.495
SQ-13	45	27.21	17.07	82.85	0.63	0.375	0.284
SQ-13	50	31.35	17.36	44.28	0.55	0.002	0.082
SQ-13	66	22.68	16.55	41.90	0.73	0.050	0.212
SQ-NU-1	o/c	19.77	16.17	40.09	0.82	0.106	0.206
SQ-NU-2	o/c	18.30	16.08	38.92	0.88	0.058	0.067
SQ-BM-2	o/c	18.58	15.98	39.61	0.86	0.028	0.063

Refer to Fig. 1 for sample locations and Fig. 4 for relationship to stratigraphic and diagenetic paleoaquifer characteristics of the Sioux Basin. Abbreviations: o/c, outcrop; ppm, parts per million; b.d., below detection limit.

than 30 are generally considered to be radiogenic. Rocks directly associated with uranium mineralization can have values in the thousands (e.g. Gulson, 1986; Holk et al., 2003). The $^{206}Pb/^{204}Pb$ ratios of drill core samples are plotted in relation to their lithologic and aquifer characteristics (Fig. 4), as samples from diagenetic paleoaquifer facies and near the unconformity are potential conduits for later fluids and therefore are more likely to have radiogenic Pb ratios if mobilization from a uranium-rich source has occurred (e.g. Holk et al., 2003). In comparison, aquitard facies should reflect regional, background common Pb values.

The majority of the samples have $^{206}Pb/^{204}Pb$ ratios that range from 17.88 to 22.68 and therefore reflect a common Pb source (Table 3; Fig. 4). Two muddy siltstone samples from drill hole SQ-13 have slightly radiogenic $^{206}Pb/^{204}Pb$ values of 27.21 and 31.35, respectively (Table 3; Fig. 4). In comparison to the very low U concentrations in drill cores SQ-3 and 6, samples from drill core SQ-13 contain higher amounts of U and anomalous Th concentrations (Table 3). The marginally radiogenic samples also contain anomalous concentrations of Mn, B, Cu, Sr, Ba, P, Fe, and Zn, suggesting scavenging of these elements and radiogenic Pb by clays in the mudstones. Thus, radiogenic Pb in drill core SQ-13 was likely produced by in-situ decay of U and Th that was mobilized locally and adsorbed onto clay mineral surfaces, and therefore it is unlikely that this radiogenic Pb originated from a more distant uranium-rich source, such as a uranium deposit.

5. Discussion

5.1. Formation of the Sioux Basin relative to other basins in the Lake Superior region

5.1.1. Lithological characteristics

The Lake Superior Quartzites are all supermature quartz arenites that contain aluminum phyllosilicates as the dominant matrix constituent. Medaris et al. (2003) suggest that low-grade metamorphism of the Sioux, Flambeau, and Baraboo Quartzites at ca. 1.6 Ga ago resulted in pyrophyllite being the dominant aluminum silicate mineral in these quartzites, in contrast to the unmetamorphosed Barron Quartzite that contains kaolinite and is north of the ca. 1.6 Ga thermal front (Fig. 2). However, in this study we find that the Sioux Basin commonly contains dickite and only minor amounts of pyrophyllite, which supports previous interpretations (e.g. Dott, 1983; Ojakangas and Weber, 1984; Medaris et al., 2003) that metamorphism of the Sioux Basin was weaker than metamorphism of the Flambeau and Baraboo Quartzites.

The Sioux Basin sandstones and mudstones contain diaspore, which is worth further mention, as its occurrence in quartz-rich sandstones is unusual and enigmatic

as diaspore is not in equilibrium with quartz except at extremely high pressures (e.g. Theye et al., 1997). Berg (1937) was the first to document the atypical occurrence of diaspore in the Sioux Basin in outcrop at Pipestone, Minnesota, and noting that it occurred in the upper part of the basin at that locality, suggested that it was a product of Cretaceous weathering. However, a weathering origin is unlikely as diaspore occurs throughout drill core SQ-3 in the Cottonwood Sub-basin, from the surface to depths of up to 280 m. The only other reported occurrence of diaspore in the Lake Superior Quartzites is from veins that also contain muscovite and pyrophyllite and locally cut the base of the Baraboo quartzite near the unconformity (Medaris et al., 2003). Based on $^{40}Ar/^{39}Ar$ ages of muscovite from these veins, Medaris et al. (2003) interpreted their formation as a result of hydrothermal activity associated with anorogenic magmatism in the region at ca. 1450 Ma, and diaspore in the Sioux Basin was assumed to have formed in a similar way.

In contrast to the interpretation by Medaris et al. (2003), petrographic textures and paragenetic relationships of diaspore to other minerals in the Sioux Basin, in combination with phase relationships in the Al_2O_3–H_2O–Si_2O system, are consistent with diaspore having formed during burial diagenesis in the Sioux Basin. During prograde metamorphism in the system Al_2O_3–H_2O–SiO_2, the first reaction should be kaolinite + 4 quartz = pyrophyllite + $2H_2O$, and with increasing temperatures the reaction kaolinite = pyrophyllite + 4 diaspore + $4H_2O$ should occur (e.g. Hemley et al., 1980; Chatterjee et al., 1984). Pyrophyllite is observed replacing kaolinite in the Sioux Basin, as predicted by the first reaction, but diaspore is never observed replacing kaolinite. Rather the opposite relationship occurs, with dickite (D2) and pyrophyllite replacing diaspore (Fig. 6b and c) indicating that the diaspore was present prior to formation of the prograde dickite (D2) and pyrophyllite. It is interesting to note that comparable paragenetic relationships among diaspore, kaolinite, and pyrophyllite have been documented in early Proterozoic quartzites of the Lorrain Formation in Ontario, where diaspore is also considered to have an early diagenetic origin (Chandler et al., 1969). Diaspore has also been noted from the western part of the Athabasca Basin in the Lazenby Lake and Locker Lake Formations, where it has been suggested that it is either detrital or a weathering product (Macdonald, 1980; Hoeve and Quirt, 1984). The presence of diaspore suggests that all these areas experienced humid and tropical paleoclimatic conditions, which may indicate that the Sioux and Athabasca basins and the Lorrain Formation were located at similar paleolatitudes during the Paleoproterozoic.

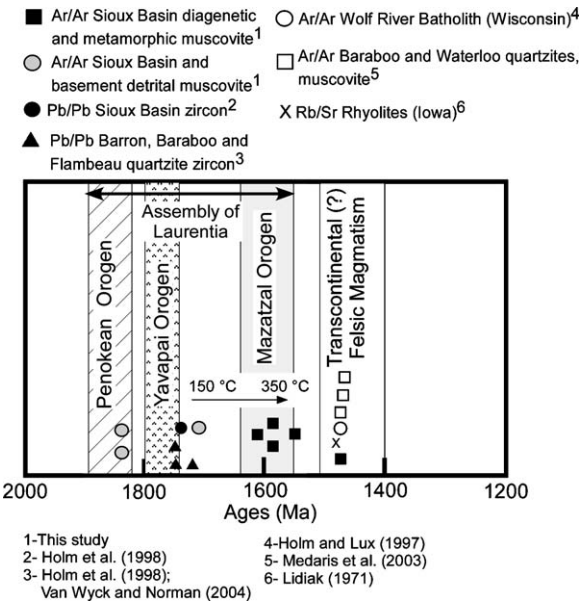

Fig. 10. Summary of geochronologic data for the Lake Superior Quartzites in relation to major tectonic events in the region. The assembly of Laurentia in the southern Lake Superior region is represented by three main orogenic events: initial amalgamation during the 1.9–1.8 Ga Penokean Orogeny (Sims et al., 1989); continued convergence from 1.8 to 1.7 Ga during the Yavapai Orogeny (Holm et al., 2005); and final assembly during the 1.6 Ga Mazatzal Orogeny (Holm et al., 1998; Romano et al., 2000; Medaris et al., 2003; Holm et al., 2005). Subsequently, 1.4–1.5 Ga felsic magmatism in the region may be part of a transcontinental event that extended from California to Labrador (e.g. Anderson, 1983; Bickford and Anderson, 1993). Temperatures represent the progression from burial diagenesis in the Sioux Basin through regional metamorphism during the Mazatzal Orogeny based on crystal chemistry and $^{40}Ar/^{39}Ar$ ages of diagenetic and metamorphic muscovite from the Sioux Basin.

5.1.2. Geochronology

The maximum age of deposition of the Sioux Basin is ca. 1730 Ma based on the youngest $^{207}Pb/^{206}Pb$ age from detrital zircons from the base of the Sioux Basin (Holm et al., 1998; Fig. 10). The other Lake Superior Quartzites have zircon populations with similar $^{207}Pb/^{206}Pb$ ages of 1714–1754 Ma (Holm et al., 1998; Van Wyck and Norman, 2004; Fig. 10). Deposition of the Lake Superior Quartzites thus postdates widespread, post-Penokean magmatism in the Lake Superior region (Holm et al., 1998; Medaris et al., 2003; Van Wyck and Norman, 2004) that is likely related to subduction of the Yavapai plate on the southern margin of Laurentia at ca. 1.8–1.7 Ga ago (Holm et al., 2005; Figs. 3 and 10). Previous geochronological studies and the results of $^{40}Ar/^{39}Ar$ dating of muscovite in this study all suggest that the Lake Superior Quartzites had a similar tectonic history, with local variations likely reflecting the proximity to the southern margin of Laurentia during

convergence and the position of the Yavapai plate during post-Penokean subduction (e.g. Holm et al., 2005).

Ar/Ar and Rb/Sr ages of 1630–1576 Ma (Dott and Dalziel, 1972; Van Schmus et al., 1993; Holm et al., 1998; Romano et al., 2000) from basement rocks underlying the deformed Flambeau and Baraboo Quartzites are thought to reflect isotopic resetting in response to deformation and low-grade metamorphism during the Mazatzal Orogeny (Holm et al., 1998; Romano et al., 2000; Medaris et al., 2003). It has been assumed (e.g. Holm et al., 1998; Medaris et al., 2003) that deformation and metamorphism of the Lake Superior Quartzites is related to the Mazatzal Orogeny, but there is no direct evidence within the quartzites, per se, to support this. In an effort to address this, Medaris et al. (2003) dated muscovite from the Baraboo and Waterloo Quartzites and whole rock samples from the Sioux Basin, expecting to obtain ages reflecting the Mazatzal Orogeny. Instead, they obtained $^{40}Ar/^{39}Ar$ ages of 1452–1467 Ma (Fig. 10) from the Baraboo and Waterloo Quartzites, which they attributed to later K-metasomatism in relation to granitic rocks associated with the ca. 1465 Ma Wolf River batholith in northeastern Wisconsin (Aldrich et al., 1959; Anderson and Cullers, 1978) that may be a local manifestation of a 1.4–1.5 Ga transcontinental magmatic event in North America (Anderson, 1983; Bickford and Anderson, 1993). From the Sioux Basin, they obtained whole rock $^{40}Ar/^{39}Ar$ ages of 1280–1370 Ma and attributed these lower ages to the fine grain size of muscovite in the samples, speculating that these finer grains had lower closure temperatures and higher rates of Ar leakage. Their results from the Sioux Basin are not surprising, as whole rock $^{40}Ar/^{39}Ar$ analysis is much less robust than dating minerals and as a consequence, attributing the ages to the grain size of muscovite when the whole rock has been analyzed can only be speculative as the Ar measured will very likely represent more than one source. In summary, Medaris et al. (2003) concluded from their studies that the muscovite + diaspore + pyrophyllite assemblage in both the Sioux and Baraboo Quartzites is younger and unrelated to the ca. 1.6 Ga thermal and tectonic front in northern Wisconsin.

In contrast, $^{40}Ar/^{39}Ar$ ages and petrographic studies of muscovite (M1 and M2) from the Sioux Basin in this study suggest that diagenetic muscovite (M1) formed during burial diagenesis at ca. 1724 Ma (Fig. 9) and lower ages from 1615 to 1543 Ma from both diagenetic and metamorphic muscovite (M1 and M2) provide the first geochronological evidence supporting 1.6 Ga Mazatzal-related deformation and metamorphism of the Lake Superior Quartzites. Furthermore, the disturbed Ar spectra, range of ages from 1724 to 1465 Ma, and variable crystallinities for muscovite (Figs. 7 and 9; Table 2) from the Sioux Basin record a complex fluid history that involved burial diagenesis followed by fluid flow and non-uniform heating up to 350 °C, in response to the ca. 1.6 Ga Mazatzal Orogeny and ca. 1.5–1.4 Ga felsic magmatism, respectively (Fig. 10). In comparison, muscovite (M0) from basement rocks underlying the Sioux Basin and detrital muscovite (M0) in well-cemented sandstones near the unconformity, retain Penokean cooling ages of ca. 1830 Ma (Fig. 10), indicating that these rocks were unaffected by the Mazatzal Orogeny, likely because of their low permeabilities. This is in contrast to reset ages of ca. 1630 Ma in basement rocks underlying the deformed quartzites in northcentral Minnesota and Wisconsin (Dott and Dalziel, 1972; Van Schmus et al., 1975; Holm et al., 1998; Romano et al., 2000), which suggests that metamorphism reached ~350 °C in these regions, which likely reflects their closer proximity to the Mazatzal Orogen and may also indicate that the basement lithologies in this area were more permeable.

5.1.3. *Correlative nature of the Sioux Basin*

The Sioux Basin and other quartzites in the southern Lake Superior region were likely part of a thick extensive wedge of clastic sedimentary rocks that were deposited during a period of cratonic stability from ca. 1750 to 1650 Ma. Renewed convergence on the southern margin of Laurentia during the Mazatzal Orogeny at ca. 1.6 Ga, resulted in variable degrees of metamorphism and deformation of the quartzites, which is reflected in $^{40}Ar/^{39}Ar$ ages of 1615–1543 Ma for muscovite from the Sioux Basin (Fig. 10). One muscovite sample from the Sioux Basin has a $^{40}Ar/^{39}Ar$ age of 1465 Ma and is similar to $^{40}Ar/^{39}Ar$ ages of 1452–1467 Ma from the Baraboo and Waterloo Quartzites (Medaris et al., 2003; Fig. 10). This suggests that thermal resetting due to felsic magmatism in the region at ca. 1450 Ma was less intense in the Sioux region, and we propose that muscovite in the Baraboo and Waterloo Quartzites may have formed during burial diagenesis, similar to muscovite in the Sioux Basin, but due to the closer proximity of these quartzites to felsic magmatism, thermal heating has completely reset their $^{40}Ar/^{39}Ar$ ages to ca. 1450 Ma. Additionally, the differences in fluid and thermal resetting of Ar in muscovite from the Lake Superior Quartzites may be related to variations in crustal strength and differential stresses, the latter being related to the position of the Yavapai plate during subduction and accretion on the southern margin of Laurentia as suggested by Holm et al. (2005).

In précis, $^{40}Ar/^{39}Ar$ ages from muscovite in the Sioux Basin provide the first geochronological evidence for

Mazatzal-related deformation and metamorphism of the Lake Superior Quartzites and support previous interpretations that the quartzites likely formed during a period of cratonic stability from 1750 to 1650 Ma (e.g. Holm et al., 1998; Medaris et al., 2003).

5.2. Mineralization potential: a comparison to the Athabasca Basin

Unconformity-related uranium deposits comprise some of the world's largest and highest-grade sources of uranium and production from these deposits accounts for approximately one-third of the world's total uranium. Current economic sources of unconformity-related uranium occur mainly in association with Paleoproterozoic basins such as the Athabasca Basin in Canada that contains the largest and highest-grade deposits of this type in the world. The economic value of unconformity-related uranium deposits therefore warrants exploration for comparable deposits in sedimentary basins that are similar in age and lithological characteristics as the Athabasca Basin. The Sioux Basin is a logical candidate to host unconformity-related uranium mineralization and warrants evaluation as such.

By assuming the Athabasca Basin represents an ideal end member for the genesis of unconformity-related uranium mineralization, we can compare certain key characteristics of the Athabasca Basin to those of the Sioux Basin to evaluate the potential of the latter. Some of these key characteristics include the diagenetic paleoaquifer characteristics, and timing and geochemistry of diagenetic fluids, as numerous studies (e.g. Garven and Freeze, 1984; Bethke, 1986; Kotzer and Kyser, 1995; Fayek and Kyser, 1997; Garven and Raffensperger, 1997; Kyser et al., 2000; Renac et al., 2002; Hiatt et al., 2003; Kyser and Hiatt, 2003) have indicated that understanding the timing, geochemical characteristics, and extent of fluids in sedimentary basins is critical for formulating genetic models and evaluating the potential of a basin to host mineralization.

The majority of the Sioux Basin is comprised of quartz arenite facies that were probably aquitards during peak diagenesis, as they were well-sorted, strongly cemented and contain very little (i.e. <5%) clay minerals. Thin, diagenetic paleoaquifers (Hiatt et al., 2003) were present, primarily near the unconformity (Fig. 4) and contain dickite (D1) and muscovite (M1) that formed during burial diagenesis. $^{40}Ar/^{39}Ar$ ages from diagenetic and metamorphic muscovite (M1 and M2) record fluid migration and heating related to the ca. 1.6 Ga Mazatzal Orogeny and ca. 1.4–1.5 Ga felsic magmatism in the region, thus indicating that the paleoaquifers remained open to fluids for at least a few 100 million years after deposition in the Sioux Basin at ca. 1730 Ma. Diagenetic paleoaquifers in the Athabasca Basin also remained open to fluids for a similar length of time as indicated by a Rb/Sr isochron age of 1477 ± 57 Ma for diagenetic illite (Kotzer et al., 1992; Kotzer and Kyser, 1995). However, in comparison to the Sioux Basin, the Athabasca Basin diagenetic paleoaquifers were quite extensive, resulting in widespread diagenetic alteration that formed a variety of clay minerals, including kaolinite, dickite, illite, magnesiofoitite, and sudoite, both regionally and in association with unconformity-related uranium deposits (e.g. Hoeve and Quirt, 1984; Kotzer and Kyser, 1995; Kyser et al., 2000).

The stable isotopic composition of dickite and muscovite in the Sioux Basin indicate that pore waters that were present in the Sioux Basin during diagenesis had temperatures of 150–200 °C and $\delta^{18}O$ and δD values of +0.3 to +5.2‰ and −28 to −46‰, respectively, consistent with a dominantly meteoric source and possibly a small contribution from evaporated seawater (Fig. 8). In comparison, peak diagenetic fluids associated with diagenetic alteration and uranium mineralization in the Athabasca Basin have similar $\delta^{18}O$ and δD fluid values and temperatures as fluids in equilibrium with diagenetic muscovite (M1) from the Sioux Basin (Fig. 8). These similarities suggest that during peak diagenesis, fluids in the Sioux Basin may have had the appropriate chemical and physical characteristics (i.e. temperature) for leaching and transporting uranium. However, in contrast to the radiogenic leachable Pb in the Athabasca Basin (Holk et al., 2003), the common Pb isotopic compositions of leachable Pb in the Sioux Basin sandstones (Table 3) provide no evidence for a uranium-rich source.

Based on comparisons with the uranium-rich Athabasca Basin, the mineralization potential of the Sioux Basin can be summarized into positive and negative indicators for hosting unconformity-related uranium mineralization. The results of our study are biased towards the northeastern portion of the Cottonwood Subbasin since this is the only part of the basin that has drill core available for study. The positive indicators for uranium mineralization include:

1. Both the Sioux and Athabasca Basins are ca. 1.7 Ga Paleoproterozoic basins that are dominated by supermature quartz arenites deposited mainly in a fluvial environment, and overlie deformed and metamorphosed basement rocks on a well-developed paleoregolith at the unconformity.
2. The Sioux Basin has comparable temperatures and isotopic compositions of diagenetic fluids as those

that were present in the Athabasca Basin during peak diagenesis and unconformity-related uranium mineralization (Fig. 8).
3. $^{40}Ar/^{39}Ar$ ages for muscovite indicate that parts of the Sioux Basin was open to fluids to at least ca. 1450 Ma, thus indicating there was ample time for diagenetic reactions that are requisite for mineralization.

The negative indicators include:

1. Thin, segmented, diagenetic paleoaquifers indicate that fluid flow was probably localized in the Sioux Basin and not on the basinal scale required to promote unconformity-related uranium mineralization.
2. Leachable Pb from sandstones in the Sioux Basin is non-radiogenic, indicating that mobilization of radiogenic Pb within the Sioux Basin from a uranium-rich source has not occurred.
3. Low-grade metamorphism at ca. 1.6 Ga has decreased the permeability of the sandstones, thereby limiting later diagenetic reactions that could promote mineralization.
4. The appropriate traps for uranium deposition, which in the Athabasca Basin include reducing lithologies in the basement rocks (e.g. Hoeve and Quirt, 1984; Kotzer and Kyser, 1995; Fayek and Kyser, 1997), may not be present in the Sioux Basin.

6. Summary

$^{40}Ar/^{39}Ar$ ages from 1615 to 1543 Ma for muscovite in the Sioux Basin provide the first geochronological evidence for ca. 1.6 Ga Mazatzal-related deformation and metamorphism of the Lake Superior Quartzites, which has been previously assumed on the basis of $^{40}Ar/^{39}Ar$ ages in basement rocks beneath the more deformed quartzites in northcentral Minnesota and Wisconsin (Dott and Dalziel, 1972; Van Schmus et al., 1975; Holm et al., 1998; Romano et al., 2000). In terms of the uranium mineralization potential of the Sioux Basin, this study suggests that although the Sioux Basin has similar characteristics to the uranium-rich Athabasca Basin, there are other critical characteristics, such as the limited extent of the diagenetic paleoaquifers and absence of radiogenic Pb, that downgrade the potential of the Sioux Basin to host significant unconformity-related uranium deposits.

Acknowledgements

We would like to thank Cameco Corporation, in particular Garth Drever, Ted O'Connor, Vlad Sopuck, and Dave Thomas for logistical and geological advice. Nick Geboy is thanked for his friendly and capable assistance in the field. This research is part of a Ph.D. thesis by A.J.H., which has been funded by a Collaborative Research and Devolopment Grant between NSERC and Cameco Corp., Discovery Grants, Ontario Innovation Trust and Canadian Foundation for Innovation Grants to TKK and a University of Wisconsin-Oshkosh Faculty Development grant to EEH. We thank Paul Polito and Paul Alexandre for their advice and stimulating discussions on basin research over the course of this study. Kerry Klassen, Don Chipley, April Vuletich and Doug Archibald kindly provided technical assistance and instruction for geochemical analyses in the Queen's Facility for Isotope Research (QFIR).

References

Aldrich, L.T., Wetherill, G.W., Bass, M.N., Compston, W., Davis, G.L., Tilton, G.R., 1959. Mineral Age Measurements, vol. 58, Carnegie Institute Washington Year Book, pp. 246–247.

Anderson, J.L., Cullers, R.L., 1978. Geochemistry and evolution of the Wolf River Batholith, a Late Precambrian rapakivi massif in north Wisconsin, USA. Precambrian Res. 7, 287–324.

Anderson, J.L., 1983. Proterozoic anorogenic granite plutonism of North America. In: Medaris Jr., L.G., Byers, C.W., Mickelson, D.M., Shanks, W.C. (Eds.), Proterozoic Geology: Selected Papers from an International Proterozoic Symposium, vol. 161. Geol. Soc. Am. Mem, pp. 133–154.

Annesley, I.R., Madore, C., Shi, R., 1995. Revision mapping/integrated geology. Wollaston, EAGLE Project: Segment 1 Report, Saskatchewan Research Council, Publication, no., R-1230-16-C-95, p. 132.

Annesley, I.R., Madore, C., Shi, R., 1996. Wollaston EAGLE Project, Revision mapping/integrated geology. Wollaston EAGLE Project: Segment 2 Report, Saskatchewan Research Council, Publication no. R1420-5-C-96, p. 184.

Ansfield, V.J., Stach, R.L., 1981. Uranium ore possibilities associated with the unconformity beneath the Sioux Quartzite, South Dakota. Geol. Soc. Am. Abstr. Prog. 13, 189.

Baldwin, W.B., 1951. Geology of the Sioux Formation. Unpublished Ph.D. Thesis. Columbia University, p. 167.

Bickford, M.E., Anderson, J.L., 1993. Middle Proterozoic magmatism. In: Reed Jr., J.C., Bickford, M.E., Houston, R.S., Link, P.K., Rankin, D.W., Sims, P.K., Van Schmus, W.R. (Eds.), Precambrian-Conterminous U.S., The Geology of North America C-2. Geol. Soc. Am., Boulder, Colorado, pp. 281–292.

Berg, E.L., 1937. An occurrence of diaspore in quartzite. Am. Miner. 22, 997–999.

Bethke, C.M., 1986. Hydrologic constraints on the genesis of the Upper Mississippi Valley mineral district from Illinois Basin brines. Econ. Geol. 81, 233–248.

Chandler, F.W., Young, G.M., Wood, J., 1969. Diaspore in Early Proterozoic quartzites (Lorrain Formation) of Ontario. Can. J. Earth Sci. 6, 337–340.

Chatterjee, N.D., Johannes, W., Leistner, H., 1984. The system CaO-Al_2O_3-SiO_2-H_2O: new phase equilibria data, some calculated

phase relations, and their petrological applications. Contrib. Mineral. Petrol. 88, 1–13.

Clayton, R., Mayeda, T.K., 1963. The use of bromine pentafluoride in the extraction of oxygen from oxides and silicates for isotopic analysis. Geochim. Cosmochim. Acta 27, 43–52.

Craig, 1961. Isotopic variations in meteoric waters. Science 133, 1702–1703.

Dahlkamp, F.J., 1978. Geologic appraisal of the Key Lake U-Ni deposits, northern Saskatchewan. Econ. Geol. 73, 1430–1449.

Dahlkamp, F.J., 1993. Uranium Ore Deposits. Springer-Verlag, Berlin, p. 460.

Dallmeyer, R.D., 1979. $^{40}Ar/^{39}Ar$ dating; principles, techniques, and applications in orogenic terranes. In: Jaeger, E., Hunziker, J.C. (Eds.), Lectures in Isotope Geology. Springer-Verlag, Germany, pp. 77–104.

Dott, R.H.J., 1983. The Proterozoic red quartzite enigma in the north-central United States: resolved by plate collision? Geol. Soc. Am. Mem. 160, 129–141.

Dott, R.H.J., Dalziel, I.W.D., 1972. Age and correlation of the Precambrian Baraboo Quartzite of Wisconsin. J. Geol. 80, 552–568.

Ehrenberg, S.N., Aagaard, P., Wilson, M.J., Fraser, A.R., Duthie, D.M.L., 1993. Depth-dependent transformation of kaolinite to dickite in sandstones of the Norwegian continental shelf. Clay Miner. 28, 325–352.

Eiler, J.M., Valley, J.W., 1994. Preservation of premetamorphic oxygen isotope ratios in granitic orthogneiss from the Adirondack Mountains, New York. Geochim. Cosmochim. Acta 58, 5525–5535.

Eye, F., Gauthier-Lafaye, F., Lillie, F., Schumacher, F., Weber, F., 1983. Le gisement d'uranium de Cluff D (Saskatchewan, Canada) Etude structurale et pétrographique. In: Pagel, M. (Ed.), Les gisements d'uranium lies spatialement aux discordances, vol. 1. le Centre de Recherches sur la Géologie de l'Uranium, Memoire, pp. 97–113.

Fayek, M., Kyser, T.K., 1997. Characterization of multiple fluid flow events and rare-earth-element mobility associated with formation of unconformity-type uranium deposits in the Athabasca Basin, Saskatchewan. Can. Miner. 35, 627–658.

Fleck, R.J., Sutter, J.F., Ellito, D.H., 1977. Interpretation of discordant $^{40}Ar/^{39}Ar$ age-spectra of Mesozoic tholeiites from Antarctica. Geochim. Cosmochim. Acta. 41, 15–32.

Fogwill, W.D., 1985. Canadian and Saskatchewan uranium deposits: compilation, metallogeny, models, exploration. In: Sibbald, T.I.I., Petruk, W. (Eds.), Geology of Uranium Deposits, CIM special volume 32, pp. 3–19.

Garven, G., Freeze, R.A., 1984. Theoretical analysis of the role of groundwater flow in the genesis of stratabound ore deposits: I. Mathematical and numerical models. Am. J. Sci. 284, 1085–1124.

Garven, G., Raffensperger, J.P., 1997. Hydrogeology and geochemistry of ore genesis in sedimentary basins. In: Barnes, H.L. (Ed.), Geochemistry of Hydrothermal Ore Deposits, third ed. John Wiley and Sons, NY, pp. 125–190.

Gilg, H.A., Sheppard, M.F., 1996. Hydrogen isotope fractionation between kaolinite and water revisited. Geochim. Cosmochim. Acta 60, 529–533.

Goldich, S.S., Nier, A.O., Baadsgaard, H., Hoffman, J.H., Krueger, H.W., 1961. The Precambrian geology and geochronology of Minnesota. Minn. Geol. Surv. Bull. 41, 193.

Greenburg, J.K., Brown, B.A., 1984. Cratonic sedimentation during the Proterozoic: an anorogenic connection in Wisconsin and the Upper Midwest. J. Geol. 92, 159–171.

Gulson, B., 1986. Lead isotopes in mineral exploration. In: Developments in Econ. Geol., vol. 23. Elsevier, NY, p. 245.

Hanes, J.A., 1991. K-Ar and $^{40}Ar/^{39}Ar$ geochronology: methods and applications. In: Heaman, L., Ludden, J.N. (Eds.), Applications of Radiogenic Isotope Systems to Problems in Geology; Short Course Handbook, vol. 19. Mineralogical Association of Canada, Toronto, Canada, pp. 27–57.

Hiatt, E.E., Kyser, K., Dalrymple, R.W., 2003. Relationships among sedimentology, stratigraphy, and diagenesis in the Proterozoic Thelon Basin, Nunavut, Canada: implications for paleoaquifers and sedimentary-hosted mineral deposits. J. Geochem. Explor. 80, 221–240.

Hills, J.H., Richards, J.R., 1976. Pitchblende and galena ages in the Alligator Rivers region, Northern Territory, Australia. Mineralium Deposita 11, 133–154.

Hemley, J.J., Montoya, J.W., Marinenko, J.W., Luce, R.W., 1980. Equilibria in the system Al_2O_3-SiO_2-H_2O and some general implications for alteration/mineralization processes. Econ. Geol. 75, 210–228.

Hoeve, J., Sibbald, T.I.I., 1978. On the genesis of Rabbit Lake and other unconformity-ype uranium deposits in northern Saskatchewa, Canada. Econ. Geol. 73, 1450–1473.

Hoeve, J., Quirt, D., 1984. Mineralization and Host Rock Alteration in Relation to Clay Mineral Diagenesis and Evolution of the Middle-Proterozoic Athabasca Basin, Northern Saskatchewan, Canada. Saskatchewan Research Council Technical Report no. 187, pp. 177.

Hoeve, J., Quirt, D., 1987. A stationary redox front as a critical factor in the formation of high-grade, unconformity-related uranium ores in the Athabasca Basin, Saskatchewan. Bull. Minéralogie 110, 157–171.

Hoeve, H., Sibbald, T.I.I., Rameakers, P., Lewry, J.F., 1980. Athabasca Basin unconformity-related deposits: a special class of sandstone-type deposits? In: Ferguson, J., Goleby, A.B. (Eds.), Uranium in the Pine Creek Geosyncline. IAEA, Vienna, pp. 575–594.

Holk, G.J., Kyser, T.K., Chipley, D., Hiatt, E.E., Marlatt, J., 2003. Mobile Pb-isotopes in Proterozoic sedimentary basins as guides for exploration of uranium deposits. J. Geochem. Explor. 80, 297–320.

Holm, D., Schneider, D., Coath, C.D., 1998. Age and deformation of Early Proterozoic quartzites in the southern Lake Superior region: implications for extent of foreland deformation during final assembly of Laurentia. Geology 26, 907–910.

Holm, D.K., Van Schmus, W.R., MacNeill, L.C., Boerboom, T.J., Schweitzer, D., Schneider, D., 2005. U-Pb geochronology of Paleoproterozic plutons from the northern mid-continent, USA: evidence for subduction flip and continued convergence after geon 18 Penokean orogenesis. Geol. Soc. Am. Bull. 117, 259–275.

Hoffman, F.P., 1988. United plates of America, the birth of a craton. Annu. Rev. Earth Planet. Sci. 16, 543–603.

Hoffman, F.P., 1989. Precambrian geology and tectonic history of North America. In: Bayy, A.W., Palmer, A.R. (Eds.), The Geology of North America—An Overview, vol. A. Geological Society of America, The Geology of North America, pp. 447–512.

Karlstrom, K., Ahall, K.-I., Harlan, S.S., Williams, M.L., McLelland, J., Geissman, J.W., 2001. Long-lived (1.8–1.0 Ga) convergent orogen in southern Laurentia, its extensions to Australia and Baltica, and implications for refining Rodinia. Precambrian Res. 111, 5–30.

Kendall, C., Coplen, T.B., 2001. Distribution of oxygen-18 and deuterium in river waters across the United States. Hydrol. Process. 15, 1363–1393.

Knipping, H.D., 1974. The concepts of supergene versus hypogene emplacement of uranium at Rabbit Lake, Saskatchewan, Canada. In: Formation of Uranium, Deposits. IAEA, Vienna, pp. 531–548.

Kotzer, T.G., Kyser, T.K., 1993. O, U, and Pb isotopic and chemical variations in uraninite: implications for determining the tempo-

ral and fluid history of ancient terrains. Am. Miner. 78, 1262–1274.

Kotzer, T.G., Kyser, T.K., 1995. Petrogenesis of the Proterozoic Athabasca Basin, northern Saskatchewan, Canada, and its relation to diagenesis, hydrothermal uranium mineralization and paleohydrology. Chem. Geol. 120, 45–89.

Kotzer, T.G., Kyser, T.K., Irving, E., 1992. Paleomagnetism and the evolution of fluids in the Proterozoic Athabasca Basin, northern Saskatchewan, Canada. Can. J. Earth Sci. 29, 1474–1491.

Kubler, B., 1964. Les argiles, indicateurs de métamorphismé. Rev. Inst. Franc. Petrol. 19, 1093–1112.

Kubler, B., 1968. Evaluation quantitative du métamorphisme par la critallinité de l'illite. Bull. Centre Rech., PAU-SNPA 2, pp. 385–397.

Kyser, K., Hiatt, E.E., 2003. Fluids in sedimentary basins: an introduction. J. Geochem. Explor. 80, 139–149.

Kyser, T.K., Hiatt, E.E., Renac, C., Durocher, K., Holk, G.J., Deckart, K., 2000. Diagenetic fluids in Paleo- and Meso-proterozoic sedimentary basins and their implications for long protracted fluid histories. In: Kyser, K. (Ed.), Fluids and Basin Evolution. Mineralogical Association of Canada, Ottawa, pp. 225–262.

Land, L.S., Dutton, S.P., 1978. Cementation of a Pennsylvanian deltaic sandstone: isotopic data. J. Sediment. Petrol. 48, 1167–1176.

Langford, F.F., 1974. A supergene origin for vien-type uranium ores in the light of the western Australian calcrete-carnotite deposits. Econ. Geol. 69, 516–526.

Lee, J.K.W., Onstott, T.C., Hanes, J.A., 1990. An $^{40}Ar/^{39}Ar$ investigation of the contact effects of dyke intrusion, Kapuskasing structural zone, Ontario. A comparison of laser microprobe and furnace extraction techniques. Contrib. Mineral. Petrol. 105, 87–105.

Lidiak, E.G., 1971. Buried Precambrian rocks of South Dakota. Geol. Soc. Am. Bull. 82, 1411–1420.

Little, H.W., 1974. Uranium in Canada. Report of Activities, Part A, Geological Survey of Canada, Paper 74-1A, pp. 137–139.

Longstaffe, F.J., Ayalon, A., 1990. Hydrogen-isotope geochemistry of diagenetic clay minerals from Cretaceous sandstones, Alberta, Canada: evidence for exchange. Appl. Geochem. 5, 657–668.

Ludwig, K.R., Grauch, R.I., Nutt, C.J., Nash, J.T., Frishman, D., Simmons, K.R., 1987. Age of uranium mineralization at the Jabiluka and Ranger uranium deposits, Northern Territory, Australia: New U-Pb isotope evidence. Econ. Geol. 84, 857–874.

Macdonald, C., 1980. Mineralogy and geochemistry of the sub-Athabasca regolith near Wollaston Lake. In: Sibbald, T.I.I., Petruk, W. (Eds.), Geology of Uranium Deposits. CIM Spec. vol. 32, pp. 155–158.

Medaris Jr., L.G., Singer, B.S., Dott Jr., R.H., Naymark, A., Johnson, C.M., Schott, R.C., 2003. Late Paleoproterozoic climate, tectonics, and metamorphism in the southern Lake Superior region and Proto-North America: evidence from Baraboo Interval Quartzites. J. Geol. 111, 243–257.

Mellinger, M., 1979. Quantitative clay analysis of clay minerals: An evaluation. Saskatchewan Research Council Technical Report G79-6, Saskatoon, 45 pp.

Merrihue, C., Turner, G., 1966. Potassium-argon dating by activation with fast neutrons. J. Geophys. Res. 71, 2852–2857.

Morey, G.B., 1984. Sedimentology of the Sioux Quartzite in the Fulda Basin, southwestern Minnesota. In: Southwick, D.L. (Ed.), Shorter Contributions to the Geology of the Sioux Quartzite (Early Proterozoic), Southwestern Minnesota. Minn. Geol. Surv. Report and Investigations 32, pp. 59–74.

Morton, R.D., 1976. The Western and Northern Australia Uranium deposits-exploration guides or exploration deterrents for Saskatchewan. In: Dunn, C.E. (Ed.). Uranium in Saskatchewan, Saskatchewan Geological Society Special Publication 3, pp. 211–255.

Munday, R.J., 1979. Uranium mineralization in northern Saskatchewan. CIM Bull. 72 (April), 102–111.

Ojakangas, R.W., Weber, R.E., 1984. Petrography and paleocurrents of the Lower Proterozoic Sioux Quartzite, Minnesota and South Dakota. In: Southwick, D.L. (Ed.), Shorter Contributions to the Geology of the Sioux Quartzite (Early Proterozoic), Southwestern Minnesota. Minn. Geol. Surv. Report and Investigations 32, pp. 1–15.

O'Neil, J.R., Taylor Jr., H.P., 1969. Oxygen isotope equilibrium between muscovite and water. J. Geophys. Res. 74, 6012–6022.

Polito, P.A., Kyser, T.K., Marlatt, J., Alexandre, P., Bajwah, Z., Drever, G., 2004. Significance of alteration assemblages for the origin and evolution of the Proterozoic Nabarlek unconformity-related uranium deposit, Northern Territory, Australia. Econ. Geol. 99, 113–139.

Raffensperger, J.P., Garven, G., 1995a. The formation of unconformity-type uranium ore deposits 1. Coupled groundwater flow and heat transport modeling. Am. J. Sci. 295, 581–636.

Raffensperger, J.P., Garven, G., 1995b. The formation of unconformity-type uranium ore deposits 2. Coupled geochemical modeling. Am. J. Sci. 295, 639–696.

Ramaekers, P., 1981. Hudsonian and Helikian basins of the Athabasca Region, northern Saskatchewan. In: Campell, F.H.A. (Ed.), Proterozoic Basins of Canada. Geological Survey of Canada Paper 81-10, pp. 219–233.

Renac, C., Kyser, T.K., Durocher, K., Dreaver, G., O'Connor, T., 2002. Comparison of diagenetic fluids in the Proterozoic Thelon and Athabasca Basins, Canada: Implications for protracted fluid histories in stable intracratonic basins. Can. J. Earth Sci. 39, 113–132.

Romano, D., Holm, D.K., Foland, K.A., 2000. Determining the extent and nature of Mazatzal-related overprinting of the Penokean orogenic belt in the southern Lake Superior region, north-central USA. Precambrian Res. 104, 25–46.

Ruxton, B.P., Berry, L., 1957. Weathering of granite and associated features in Hong Kong. Geol. Soc. Am. Bull. 68, 1263–1292.

Ruzicka, 1993. Unconformity-related uranium deposits. In: Kirkham, R.V., Sinclair, W.D., Thorpe, R.I., Dyke, J.M. (Eds.), Mineral Deposit Modeling. Geological Association of Canada, Special Paper 40, pp. 125–149.

Sharp, Z.D., Atudorei, V., Durakiewicz, T., 2001. A rapid method for determination of hydrogen and oxygen isotope ratios from water and hydrous minerals. Chem. Geol. 178, 197–210.

Sims, P.K., Van Schmus, W.R., Schulz, K.J., Peterman, Z.E., 1989. Tectonostratigraphic evolution of the early Proterozoic Wisconsin magmatic terranes of the Penokean Orogen. Can. J. Earth Sci. 26, 2145–2158.

Sklar, P.J., 1983. The Corson diabase; a Precambrian mafic intrusive in the Sioux Quartzite in South Dakota. Geol. Soc. Am. Abstr. Prog. 15, 210.

Sopuck, V., Wasyliuk, K., 1996. Basement-sandstone interaction, alteration patterns and metal sourcing in Athabasca unconformity uranium deposits. In: Advances in Saskatchewan Geology, Mineral, Exploration, Saskatchewan Geological Society, MinExpo '96 Symposium, Program, Abstracts, Saskatoon, Saskatchewan, pp. 44–45.

Southwick, D.L., Mossler, J.H., 1984. The Sioux Quartzite and subjacent regolith in the Cottonwood County Basin. In: Southwick, D.L. (Ed.), Shorter Contributions to the Geology of the Sioux Quartzite

(Early Proterozoic), Southwestern Minnesota. Minn. Geol. Surv. Report and Investigations 32, pp. 17–44.

Southwick, D.L., Morey, G.B., Lively, R.S., Beltrame, R.J., 1982. New Ulm Quadrangle, Minnesota. Minn. Geol. Surv. Report PGJ/F-052/82, p. 26.

Southwick, D.L., Morey, G.B., Mossler, J.H., 1986. Fluvial origin of the lower Proterozoic Sioux Quartzite, southwestern Minnesota. Geol. Soc. Am. Bull. 97, 1437–1441.

Stacey, J.S., Kramers, J.D., 1975. Approximation of terrestrial lead isotope evolution by a two-stage model. Earth Planet. Sci. Lett. 26, 207–221.

Stach, R.L., Ansfield, V.J., Iles, D.L., 1981. Diabase occurrences associated with the Precambrian Sioux Quartzite, eastern South Dakota. Geol. Soc. of Am. Abstr. Prog. 3, 227.

Taylor, H.P., 1997. Oxygen and hydrogen isotope relationships in hydrothermal mineral deposits. In: Barnes, H.L. (Ed.), Geochemistry of Hydrothermal Ore Deposits, thirrd ed. John Wiley and Sons, New York, pp. 229–302.

Theye, T., Chopin, C., Grevel, K.D., Ockenga, E., 1997. The assemblage diaspore + quartz in metamorphic rocks: a petrological, experimental and thermodynamic study. J. Met. Geol. 15, 17–28.

Tremblay, L.P., 1982. Geology of the uranium deposits related to the sub-Athabasca unconformity, Saskatchewan. Geological Survey of Canada, Paper 81-20, p. 56.

Van Schmus, W.R., Thurman, M.E., Peterman, Z.E., 1975. Geology and Rb-Sr chronology of Middle Precambrian rocks in eastern and central Wisconsin. Geol. Soc. Am. Bull. 86, 1255–1265.

Van Schmus, W.R., Bickford, M.E., Condie, K.C., 1993. Early Proterozoic crustal evolution. In: Reed Jr., J.C., Bickford, M.E., Houston, R.S., Link, P.K., Rankin, D.W., Sims, P.K., Van Schmus, W.R. (Eds.), Precambrian: Conterminous U.S.: Geology of North America C-2, pp. 270–281.

Van Wyck, N., Norman, M., 2004. Detrital zircon ages from Early Proterozoic quartzites, Wisconsin, support rapid weathering and deposition of mature quartz arenites. J. Geol. 112, 305–315.

Wheatley, K., Murphy, J., Leppin, M., Cutts, C., and Climie, J.A., 1996. Advance in the genetic model and exploration techniques for unconformity-type uranium deposits in the Athabasca Basin. CIM Bulletin 89, Abstract no. 918.

Wilde, A.R., Wall, V.J., 1987. Geology of the Nabarlek uranium deposit, Northern Territory, Australia. Econ. Geol. 82, 1152–1168.

Wilde, A.R., Mernagh, T.P., Bloom, M.S., Hoffman, C.F., 1989. Fluid inclusion evidence on the origin of some Australian unconformity-type uranium deposits. Econ. Geol. 85, 1627–1642.

Wilson, M.R., Kyser, T.K., Mehnert, H.H., Hoeve, J.J., 1987. Changes in the H-O-Ar isotopic composition of clays during retrograde alteration. Geochim. Cosmochim. Acta 51, 869–878.

Yeh, M., 1980. D/H ratios and late-stage dehydration of shales during burial. Geochim. Cosmochim. Acta 44, 341–352.

Zotov, A., Mukhamet-Galeev, A., Schott, J., 1998. An experimental study of kaolinite and dickite relative stability at 150–300 °C and the thermodynamic properties of dickite. Am. Miner. 83, 516–524.